AGU ADVANCING EARTH AND SPACE SCIENCES

Water Resources Research

RESEARCH ARTICLE
10.1029/2023WR034975

Process-Based Atmosphere-Hydrology-Malaria Modeling: Performance for Spatio-Temporal Malaria Transmission Dynamics in Sub-Saharan Africa

Mame Diarra Bousso Dieng[1], Adrian M. Tompkins[2], Joël Arnault[1,3], Ali Sié[4], Benjamin Fersch[1], Patrick Laux[1,3], Maximilian Schwarz[5], Pascal Zabré[4], Stephen Munga[6], Sammy Khagayi[6], Ibrahima Diouf[7], and Harald Kunstmann[1,3,8]

[1]Institute of Meteorology and Climate Research (IMK-IFU), Campus Alpin, Karlsruhe Institute of Technology (KIT), Garmisch-Partenkirchen, Germany, [2]International Centre for Theoretical Physics (ICTP), Trieste, Italy, [3]Institute of Geography, University of Augsburg, Augsburg, Germany, [4]Centre de Recherche en Santé de Nouna (CRSN), Nouna, Burkina Faso, [5]Remote Sensing Solutions GmbH (RSS), Munich, Germany, [6]Kenya Medical Research Institute (KEMRI), Kisumu, Kenya, [7]Laboratoire de Physique de l'atmosphère et de l'océan Siméon Fongang (LPAOSF-ESP), Dakar, Senegal, [8]Center for Climate Resilience, University of Augsburg, Augsburg, Germany

Abstract With the goal of eradication by 2030, Malaria poses a significant health threat, profoundly influenced by meteorological and hydrological conditions. In support of malaria vector control efforts, we present a high-resolution, coupled physically-based modeling approach integrating WRF-Hydro and VECTRI. This model approach accurately captures topographic details at the scale of larvae habitats in the Nouna Health and Demographic Surveillance Systems in Sub-Saharan Africa. Our study demonstrates the proficiency of the high-resolution hydrometeorological model, WRF-Hydro, in replicating observed climate characteristics. Comparisons with in-situ local weather data reveal root mean square errors between 0.6 and 0.87 mm/day for rainfall and correlations ranging from 0.79 to 0.87 for temperatures. Additionally, WRF-Hydro's surface hydrology reproduces the seasonal and intraseasonal variability of the ponded water fraction with 96% accuracy, validated against Sentinel-1 data at a 100-m resolution. The VECTRI model demonstrates sensitivity to surface hydrology representation, particularly when comparing conceptual and detailed physical process models, for variables such as larvae density, mosquito abundance, and EIR. The model's ability to replicate the seasonality of malaria transmission aligns well with available cohort malaria data suggesting its potential for predicting the impacts of climate change on mosquito abundance and transmission intensity in endemic tropical and subtropical zones. This integrated approach opens avenues for enhanced understanding and proactive management of malaria.

Key Points:

- A coupled atmosphere-hydrology-malaria transmission model system consisting of WRF-Hydro and VECTRI is developed
- Coupled WRF-Hydro-VECTRI scheme reproduces the peak of malaria as well as the seasonal variability
- VECTRI is sensitive to the representation of mosquito breeding habitat avail-ability

Supporting Information:

Supporting Information may be found in the online version of this article.

Correspondence to:

M. D. B. Dieng,
diarra.dieng@kit.edu

Citation:

Dieng, M. D. B., Tompkins, A. M., Arnault, J., Sié, A., Fersch, B., Laux, P., et al. (2024). Process-based atmosphere-hydrology-malaria modeling: Performance for spatio-temporal malaria transmission dynamics in Sub-Saharan Africa. *Water Resources Research*, *60*, e2023WR034975. https://doi.org/10.1029/2023WR034975

Received 5 APR 2023
Accepted 24 APR 2024

Author Contributions:

Conceptualization: Mame Diarra Bousso Dieng, Adrian M. Tompkins, Benjamin Fersch, Patrick Laux, Harald Kunstmann
Investigation: Mame Diarra Bousso Dieng
Methodology: Mame Diarra Bousso Dieng, Adrian M. Tompkins, Joël Arnault, Benjamin Fersch, Patrick Laux, Ibrahima Diouf
Software: Joël Arnault
Supervision: Adrian M. Tompkins, Harald Kunstmann

1. Introduction

Malaria epidemic risk factors include pathogens, human hosts, mosquito vectors, climate, and environmental factors, which vary geographically and temporally. Sub-Saharan Africa (SSA) is severely afflicted by malaria disease with significant morbidity and mortality caused by a combination of these factors and an all-year-round transmission potential. Most infectious disease outbreaks and epidemics in SSA are connected to climate change and variability (Ayanlade et al., 2022; Moyo et al., 2023; Opoku et al., 2021; Van de Vuurst & Escobar, 2023; Yamana et al., 2016). For instance, the incidence of malaria is related to climatic factors like rainfall and temperature at specific time lags (Abiodun et al., 2016, 2017, 2018; Caminade et al., 2014; Christiansen-Jucht et al., 2015; Diouf et al., 2020; Ikeda et al., 2017; Tompkins & Ermert, 2013). Rainfall plays a crucial role in the transmission dynamics influencing various aspects of mosquito biology, habitat availability, and epidemiology. Temperatures in SSA are generally favorable to malaria transmission (Ryan et al., 2020), with an increase in temperature leading to increased biting rate (Gilles, 1993; MacLeod et al., 2015; Molineaux, 1988).

It is well established across numerous geographical contexts in SSA that when environmental and meteorological conditions favor mosquito reproduction, a significant increase in malaria infections among nearby populations can occur (Badmos et al., 2021). More precisely the number of people infected is closely linked to the amount of water available in the area, as well as the characteristics of that water (e.g., aquatic habitats, stagnant or slowly streaming fresh or salty water, Asare, Tompkins, & Bomblies, 2016; Minakawa et al., 2012; Smith et al., 2013; Yamana et al., 2016). This connection is partly because malaria vector mosquitoes utilize temporary water bodies

Validation: Mame Diarra Bousso Dieng, Ali Sié, Maximilian Schwarz, Stephen Munga, Sammy Khagayi
Visualization: Mame Diarra Bousso Dieng, Maximilian Schwarz
Writing – original draft: Mame Diarra Bousso Dieng, Joël Arnault
Writing – review & editing: Mame Diarra Bousso Dieng, Adrian M. Tompkins, Joël Arnault, Benjamin Fersch, Patrick Laux, Maximilian Schwarz, Pascal Zabré, Stephen Munga, Sammy Khagayi, Ibrahima Diouf, Harald Kunstmann

for the development of their larval stages (Getachew et al., 2020; Mwakalinga et al., 2018). The studies of Kibret et al. (2014, 2017) across malaria-endemic areas in SSA have revealed that the high transmission rate observed among residents near irrigation fields is associated with the existence of potential mosquito breeding sites. The detection of water bodies is therefore crucial in identifying malaria high-risk zones (Dambach et al., 2009, 2012; Machault et al., 2012). Typically, the mosquito's aquatic habitats are not solely based on rainfall. Local-scale hydrological conditions like soil and vegetation properties, infiltration, exfiltration, surface runoff, and evaporation, in turn, can all affect how much water is available on the land surface (Gianotti et al., 2009; Smith et al., 2013, 2020; Tompkins & Ermert, 2013). Each of these factors, independently and in combination, influences the amount and duration of surface water availability (Desconnets et al., 1996; Youssefi et al., 2022). The detection of surface water availability from current data sets is challenging, however. Wimberly et al. (2021) and Youssefi et al. (2022) mentioned that a higher spatial resolution of remote sensing data can be utilized to capture larvae and mosquito habitats.

Mathematical models are widely used to simulate the inherent and external dynamics of malaria transmission concerning climate-derived variables. They also help in simulating and predicting the spatio-temporal dynamics of epidemic risk across regional to continental scales. Complex malaria models have been introduced to simulate the African malaria vectors, designed to explicitly simulate mosquito population dynamics at a local scale (Depinay et al., 2004; Morse et al., 2005). The latter authors claimed that these malaria models have helped to facilitate the structure of existing knowledge gathered from the literature review. They have also emphasized the crucial fundamental biology of Anopheles mosquitoes, addressing areas where knowledge gaps exist. Other authors claimed that complex hydrological models can serve as valuable predictive tools for vector mosquito population dynamics. By using hybrid models (e.g., Bomblies et al., 2008; Jiang et al., 2021; Tokarz & Novak, 2018; Yamana & Eltahir, 2010), researchers have looked for suitable places for mosquito vector growth to explicitly represent the mechanistic relationships between observed rainfall, mosquito populations, and the subsequent response in malaria transmission. The suitable breeding sites of Anopheles mosquitoes have been simulated with high accuracy and most of the environmental factors have been considered. The work of Asare, Tompkins, and Bomblies (2016) integrated two basic surface hydrology models to replicate the sub-seasonal changes in fractional water coverage. However, a coupling framework consisting of high-resolution atmospheric-terrestrial hydrology modeling with the integration of satellite-derived land use information has not so far been used in analyses of disease vectors like Malaria.

This study aims to determine the influence of three distinct surface hydrology representations, environmental and climate-sensitive driver factors on malaria incidence in SSA. We explore an approach based on a coupled high-resolution atmospheric- and terrestrial model system (WRF-Hydro, Gochis et al., 2018) to improve the treatment of the temporary water bodies used by mosquitoes for breeding. It includes the statistics of ponds aggregated from remote sensing data (Sentinel-1) to evaluate those simulated in WRF-Hydro and two simple local offline hydrological schemes in VECTRI (Tompkins & Ermert, 2013) utilized as benchmarks. Using this coupled model development helps to create a framework (WRF-Hydro plus VECTRI) that allows an explicit representation of the spatiotemporal hydrological and climatological determinants of malaria transmission, exemplarily shown here for the Health and Demographic Surveillance Systems (HDSS) site regions of Nouna in Burkina Faso. To that end, we have conducted a suite of sensitivity experiments to calibrate soil parameters, aiming to generate more accurate estimates of surface water, malaria vectors, and transmission dynamics. In the following, Section 2 discusses the study area and the description of the models, followed by the methods and experimental setup, forward operator, and temporary pond fraction technique. The data collection is given in Section 3. In Section 4, the results are presented and discussed. The discussions and conclusions are given in Sections 5 and 6, respectively.

2. Study Area and Field Data

2.1. Study Area

Our modeling approach is exemplarily setup, tested, and validated for the SSA region around Nouna in Burkina Faso. Nouna Town (Figure 1c) is located in the northwestern part of Burkina Faso in the Province of Kossi (Figure 1b) with a current population of about 30,000 inhabitants. It lies between latitude 27.43°N and 29.20°N and longitude 94.42°E and 95.35°E. The Center de Recherche en Santé de Nouna (CRSN)'s research area, the so-called Nouna Health and Demographic Surveillance System covers currently 124,957 inhabitants (CRSN,

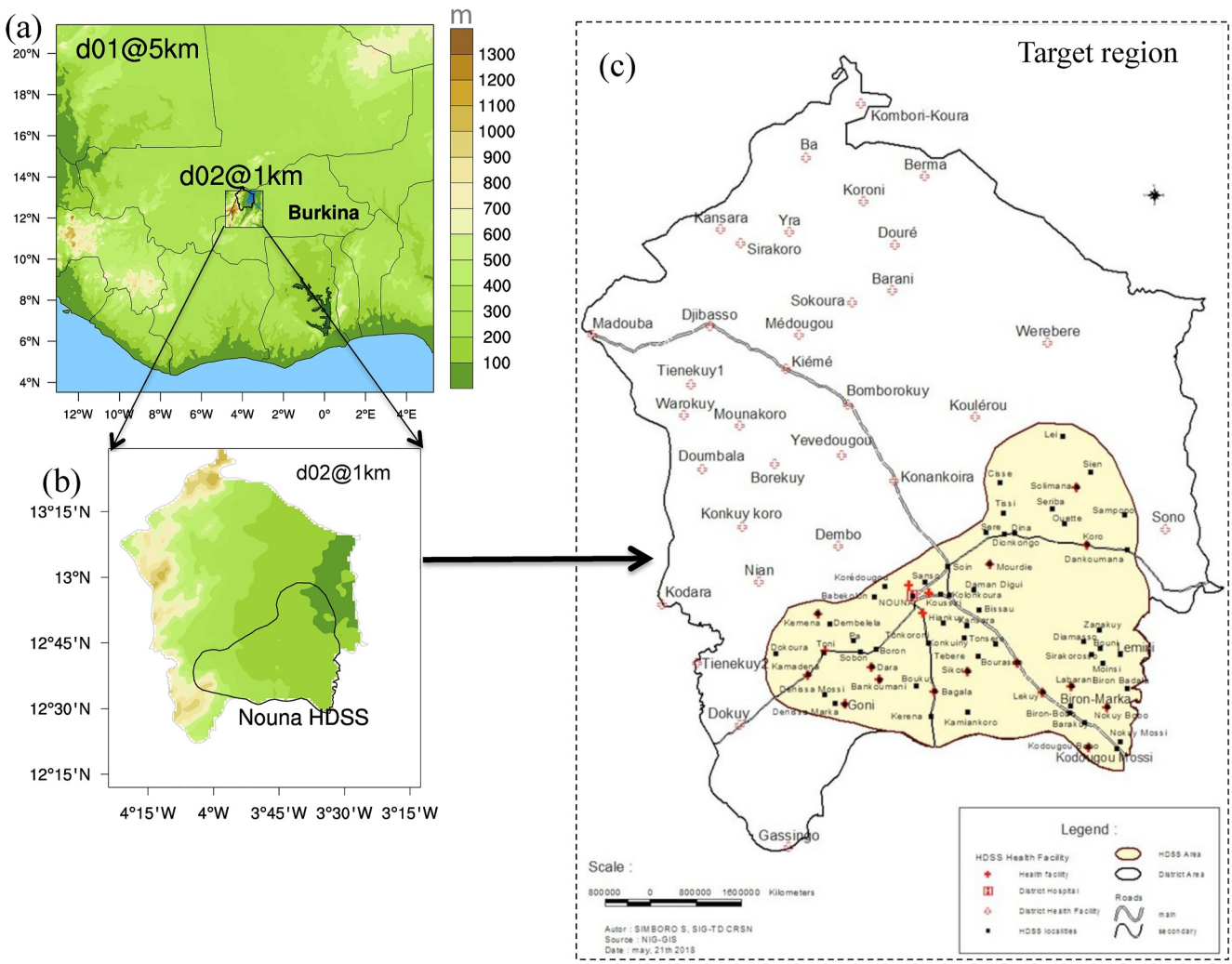

Figure 1. (a) The terrain elevation map of the 5-km resolution WRF model nested grid domains (d01). (b) WRF-Hydro has the same settings as WRF, except the inner domain (d02, 1 km) is coupled with a routing subgrid in WRF-Hydro (100 m). (c) Geographic locations of Nouna HDSS. The Nouna HDSS is located within the Nouna health district area in northwest Burkina Faso in the Kossi province, 300 km from the capital city, Ouagadougou.

2022) distributed in 15,014 households, settled over 1.775 km^2. This area is a dry orchard Savannah, populated almost exclusively with subsistence farmers of various ethnic groups. The area has a sub-Saharan climate (one rainy season usually lasting from July to September), with a mean annual rainfall of 796 mm (range 483–1,083 mm) over the past five decades and overall high temperatures throughout the year, peaking in April/May. This zone was chosen as the study area because malaria is frequent throughout the year in this district (Sie et al., 2010), with average malaria cases ranging from 279 in 2012 to 2,817 in 2016. From 2013 to 2020, the Nouna part of the Sahelo-Sudanese zones accounted for 59% of total malaria cases (Sangaré et al., 2022). Being part of the HDSS, Nouna Hospital has been equipped with diagnostic and treatment facilities for malaria and it serves as a reporting center for malaria incidence under the International Network for the Demographic Evaluation of Populations and Their Health in Developing Countries (INDEPTH) (Hondula et al., 2012; Sauerborn, 2017). Agriculture is the primary economic driver and most of the population in the district is engaged in agricultural activity. The public health facilities include one hospital and 17 health centers. The district is one of the malaria-endemic districts in the region. Numerous initiatives have been implemented in addition to quick diagnosis and treatment to prevent and control the disease. Previous studies have examined clinical research, epidemiology, health economics, and health systems research areas (Diboulo et al., 2016; Ndugwa et al., 2008; Sié et al., 2008).

2.2. Field Data

- *Population density:*
  Gridded estimates of the human population in Africa were used to evaluate the number of individuals falling within areas climatically suitable for malaria transmission. This data set is based on the 2020 Gridded Population of the World, Version 4 (GPWv4, GPWv4: Population Density, Revision 11 (2018). It relies on counts that align with national censuses and population registrations. All population data sets were at a resolution of 30 arc seconds (around 1 km at the equator) with results aggregated to the continental and country level.
- *Epidemiological data:*
  Data sources are useful for generating meaningful statistics regarding malaria; they must be thorough, accurate, relevant, and/or representative, and available promptly. This is not the case in many African countries (Nachega et al., 2012). Eight years (2013–2020) of malaria cases with strict quality control operated by the National Health Data Warehouse or ENDOS-BF (Burkina Faso ministry data system) were obtained. The data was collected using both active and passive surveillance methods which comprised several blood samples collected and tested positive either for Plasmodium vivax or Plasmodium falciparum infection or mixed infection. The data have been classified into age, confirmed and suspected cases, and simple and severe cases. In Figure S1 (Supporting Information S1), only total confirmed severe and simple cases have been represented and considered in this study. We observed higher simple cases than severe for all age categories mainly between the ages of 1–4 years. As already mentioned by the World Health Organization (WHO, 2018), Africa accounts for 90% of global malaria cases, with over 75% affecting children and expectant mothers. In our analysis, both simulated and reported malaria time series were standardized over their respective periods to show anomalies. The standardized value was calculated using the following formula:

$$\text{Standardized value} = \frac{X - \mu}{\delta} \tag{1}$$

where $X =$ the value of an observation/simulation, $\mu =$ the mean value and $\delta =$ the standard deviation.

- *Meteorological data sets:*
  The meteorological data consists of daily rainfall, daily minimum and maximum temperature, and relative humidity records collected from weather stations of the Burkina Faso Weather Service. In addition, the reference observation-based data set used in this study is the Climate Hazards Group Infrared Precipitation from 2000 to 2020 and daily maximum and minimum temperature data with Stations (CHIRPS, Funk et al., 2014, CHIRTS, Funk et al., 2019) from 2000 to 2016 available at 0.05° spatial resolution.
- *Surface water occurrence from satellite remote sensing:*
  Satellite remote sensing has attracted a lot of attention in the past two decades, it can be used as an opportunity for validating model outputs due to direct observations of various hydrological variables as well as large geographical and temporal coverage (Jiang & Wang, 2019; Khaki, 2023; Meyer Oliveira et al., 2021). We used the monthly surface water occurrence maps and the surface water dynamics from Sentinel-1 data during 2015–2020 with a spatial resolution of 10 m (later aggregated to model resolution at 100 m). The data were processed into calibrated, topographically normalized backscatter images. These preprocessed images were classified into binary water body maps using scene-dependent thresholds. These thresholds were determined based on existing geospatial information of permanent water areas, obtained from the Global Surface Water Explorer (Pekel et al., 2016). Monthly surface water composites were created from the individual classified scenes. Additionally, all unique classified scenes were used to produce a surface water dynamics layer representing the percentage of water occurring in each pixel - relative to the number of valid observations. The product represents a measure of the changing spatial extent of water bodies (permanent vs. seasonal water bodies) following Steinbach et al. (2021). Post-processing included the removal of false positives (mainly radar shadows) by using the Multi-resolution Valley Bottom Flatness index (Gallant & Dowling, 2003). This results in surface water dynamics representing the percentage of water occurring in each pixel from 2015 to 2020 (Figure 2). To assess how strongly the Sentinel 1 products corresponded to our model outputs, we compared pixel-wise area averages aggregated to the land resolution (100 m).

10.1029/2023WR034975

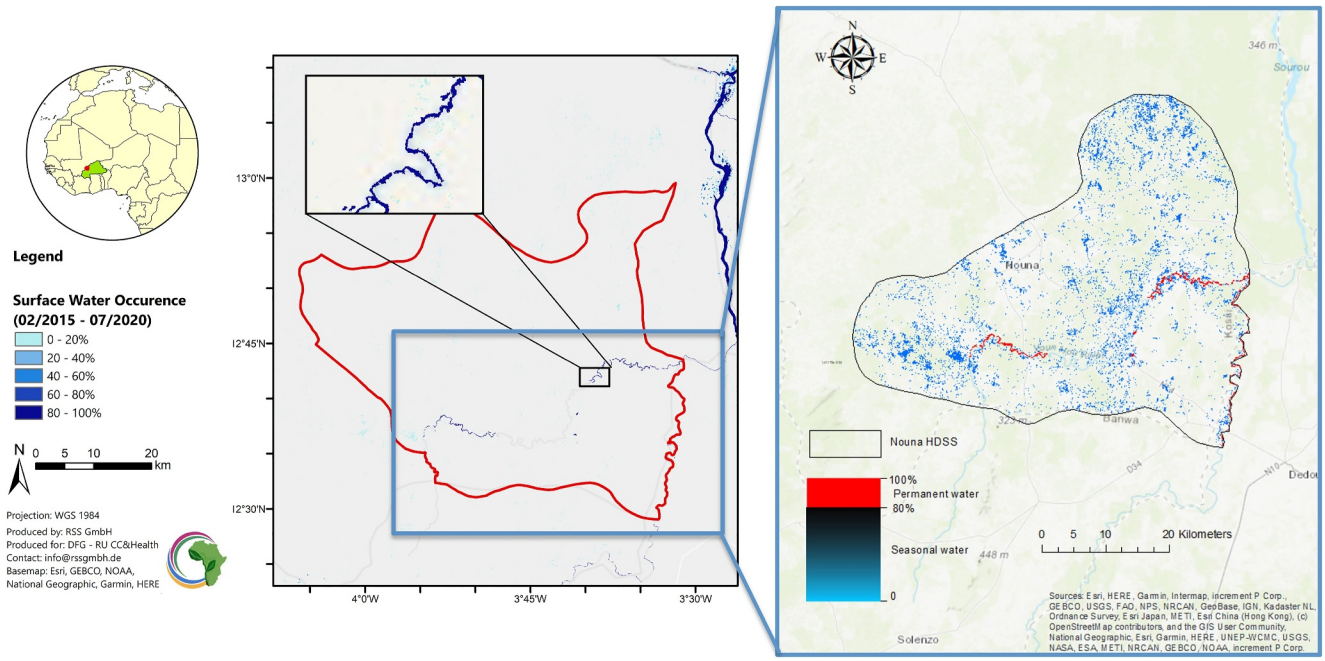

Figure 2. Surface water dynamics layer representing the percentage of water occurring in each pixel from 2015 to 2020 over Nouna HDSS.

3. Models Description and Numerical Experiment Design

Figures 3 and 4 visualize the conceptual schematic and the coupling of model components. Three distinct models are employed in this study: 1: a regional atmospheric model (WRF-ARW) for the dynamical downscaling of global reanalyzes to the target resolutions of 5 and 1 km, 2: a hydrologically enhanced land surface model (WRF-Hydro) to simulate the relevant reservoirs upon and below the land surface, and 3: a dynamical transmission model for vector-based diseases (VECTRI). Before each model runs, a 3-month spin-up period is performed to

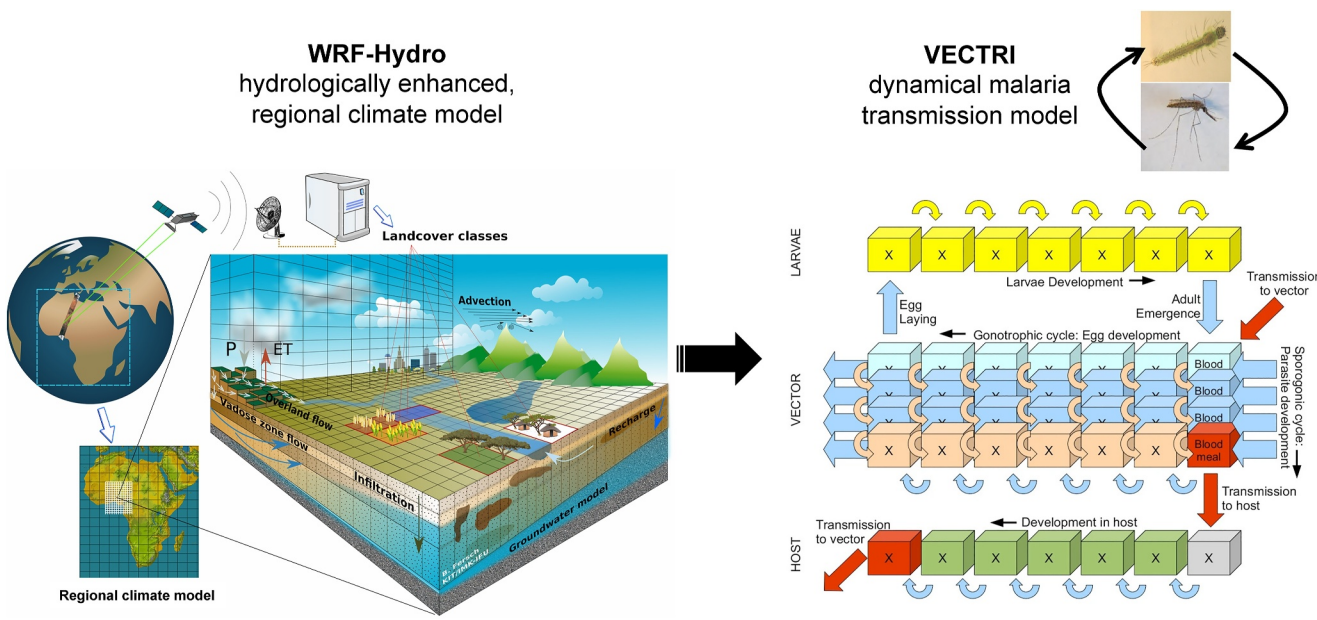

Figure 3. Fully-coupled WRF-Hydro and VECTRI model coupling framework. The left part of the figure (WRF-Hydro) illustrates the fully coupled high-resolution joint atmospheric-terrestrial hydrology modeling and integration of satellite-derived land use information. The right part illustrates the schematic of the VECTRI model (larvae status, vector state, and host infective state) obtained from Tompkins and Ermert (2013).

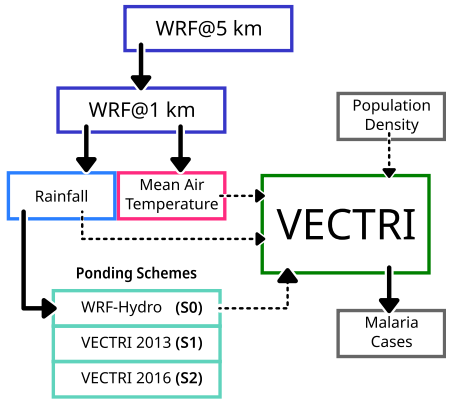

Figure 4. Workflow for the joint climate–hydrology-malaria modeling. The dashed lines represent the input data streams for VECTRI. Three different schemes are employed to describe surface water ponding (S0, S1, S2). In our experiment, (a) the climate parameters (blue and red): daily mean temperature and rainfall at 0.1° × 0.1° resolution; (b) the surface hydrological data set (green): three different estimated ponded water (PW) and (c) the population density (gray) from 2000 to 2020 are used as inputs to the VECTRI model (dark green) for the simulation. The first PW (Scheme S0) is derived from WRF-Hydro itself, whilst in the second and the third (scheme S1 and S2), the rainfall from WRF at 1 km resolution drives the VECTRI puddle model. The population density at 1 km resolution is based on the 2020 Gridded Population of the World, Version 4 (GPWv4, Gridded Population of the World, Version 4 (GPWv4): Population Density, Revision 11 (2018).

ensure that all three models reach equilibrium. In the following, the models and their configurations are briefly described.

3.1. Climate Modeling

The regional climate model Weather Research and Forecasting Model (WRF-ARW) has been used to provide detailed information on climatic conditions such as precipitation, relative humidity, maximal and minimal air temperature, and wind speed at the local scale required for modeling malaria. The WRF-ARW model (V4.0) is a time-split non-hydrostatic atmospheric model and is the most widely applied mesoscale numerical weather prediction model. It is widely used in the study of land-atmosphere interactions (Constantinidou et al., 2020), dynamical downscaling (Laux et al., 2021), weather and climate research (Igri et al., 2018). The ability of WRF to resolve strongly nonlinear small-scale phenomena such as stratiform precipitation and convective precipitation (Klein et al., 2015) makes it suitable for the coupling study of atmospheric and hydrological processes. Detailed information about WRF can be found in Skamarock et al. (2008). Optimal physical parameterization settings for the West African Region were obtained under the West African Science Service Center on Climate Change and Adapted Land Use (est African Science Service Center on Climate Change and Adapted Land) project (Heinzeller et al., 2018). Table 1 lists the model setup. The initial and lateral boundary conditions of the model were acquired from the fifth generation ERA5 reanalysis (30 km) of the European Centre for Medium-Range Weather Forecasts (Hersbach et al., 2020).

3.2. Land Surface Modeling

WRF offers several options for land surface schemes that can be used to describe the heat, moisture, and momentum exchange across the surface-atmosphere interface. For the fully coupled WRF/WRF-Hydro simulation, Noah Multi-Parameterization (Noah-MP) LSM was the land model used. The Noah-MP land surface model (Niu et al., 2011) is an enhanced version of the Noah land surface model (Noah LSM, Ek et al. (2003)) coupled with WRF, and introduces a framework for multiple schemes. Due to the enhancement of biophysical and soil freeze-thaw processes, these LSMs have been widely used and the most common land surface process module configuration applied in WRF studies in SSA (Arnault et al., 2016; Campbell et al., 2019; Diaz et al., 2015; García-Ortega et al., 2020; Klein et al., 2015). Noah LSM, and especially Noah-MP, account for the column hydrological processes (i.e., through fall, evapotranspiration, soil infiltration, vertical soil water movement, and accumulation of both surface and underground runoff). The required input fields passed from the Noah-MP to the WRF-Hydro (see the section below) routing modules include maximum soil moisture (SM) for each soil type, infiltration capacity excess, lateral surface hydraulic conductivity for each soil type, and the SM content for each soil layer.

Table 1
WRF Physical Parameterizations Used in This Study

Physics categories	Selected option	Reference
Microphysics	WRF Single-Moment 6-class scheme (WSM6)	Hong and Lim (2006)
Cumulus parametrization	None	
Planetary boundary layer	Asymmetric Convection Model version 2 (ACM2)	Pleim (2007)
Land surface model	Noah-MP	Niu et al. (2011)
Longwave radiation	Rapid Radiative Transfer Model (RRTM)	Mlawer et al. (1997)
Shortwave radiation	Dudhia	Dudhia (1989)

3.3. Hydrological Modeling

WRF-Hydro is a comprehensive atmosphere-hydrology model system specifically designed to enable the coupling of land-surface modeling with WRF (Arnault et al., 2016; Kerandi et al., 2018). In this study, we apply version 5.0 with a particular interest in one major improvement in WRF-Hydro, which consists of allowing excess infiltration to remain as ponded water (PW) (100 m resolution) for subsequent lateral redistribution in combination with precipitation in the following model time step (Yucel et al., 2015). This integrated model system requires high-resolution topography and channel networks to depict hydrological processes impacting terrestrial water accurately. This includes lateral water flows in the subsurface, overland, and rivers, which enhances the representation of land-atmosphere feedback. Such improvements, as demonstrated by, for example, Lahmers et al. (2019) and Arnault et al. (2021), addressed questions regarding land use's influence on climate change and water availability. Here, WRF-Hydro allowed benefiting from several remotely sensed data sources to predict the probability of pond presence. WRF-Hydro utilizes the high-resolution digital elevation model (DEM, 30 s), providing a high-quality terrain data set derived from Shuttle Radar Topography Mission data. In this study, Noah-MP (see Section 3.2) is parameterized over a 1 km × 1 km grid, while WRF-Hydro water routing processes are run over a 100 m × 100 m grid.

3.4. Malaria Modeling

VECTRI features a spatially explicit representation of Anopheles mosquito population interactions with humans and natural environments. It provides an organized, structured, and process-based approach representing the environmental causes of malaria transmission. VECTRI (VECTor borne disease community model of International Center for Theoretical Physics, TRIeste, Tompkins & Ermert, 2013) is a grid cell distributed dynamical model (Figure 2). It accounts for the temperature and rainfall influences on the parasite and vector life cycles which are finely resolved to correctly represent the delay between the rains and the malaria season. Most relationships are taken from the literature for the *Anopheles gambiae* vector and the *Plasmodium faciparum* parasite species. The model accounts for the population density in calculating daily biting rates. It is designed for regional to continental scales at high spatial resolutions of around 1–10 km using a daily integration time step. VECTRI is just one example of several mechanistic models for malaria transmission. VECTRI is the only model that accounts for climate and population density and includes a simple representation of immunity (Laneri et al., 2010; Tompkins & Thomson, 2018). It also has two different parameterizations of the local surface hydrology which will be introduced below. The model has been used for both seasonal forecasting purposes and investigating the impact of climate change on malaria transmission (Caminade et al., 2014; Colón-González et al., 2021; Tompkins et al., 2019). The VECTRI model fits the spatial scales of the Nouna (≈700 km^2) region. This study applies to version 1.9 of VECTRI.

3.5. Experiment Design: Joint Hydro-Climate-Malaria Modeling

Figure 3 summarizes the components and steps of the high-resolution climate to malaria modeling chain including the coupling with the atmospheric-hydrological model WRF/WRF-Hydro (Gochis et al., 2018) and the dynamical Malaria transmission model VECTRI (Tompkins & Ermert, 2013). The atmospheric model domain is centred at 3.87°W, 12.61°N with a total of 400 × 400 grid points at 5 km spatial resolution (Figure 1a). It is set up in a one-way nesting approach with two domains: the outer domain d01, referred to as WRF@5 km, covers most of West Africa (37°W to 48°E, 18°S to 36°N) (see Figure 1) at a resolution of 0.05° (5 km, 400 × 400), and a nested inner domain d02, referred to as WRF@1 km, covering a region centred on Nouna HDSS (27.5°W to 27.5°E, 7.5°S, 27.5°N) at a resolution of 0.01° (1 km, 200 × 200). Next, the WRF model (1 km) generates atmospheric input data for calibrating hydrological processes. Afterwards, rainfall, temperature, and population density are used as driving data for VECTRI runs over the domain of 1 km by processing the two surfaces hydrological model provided by VECTRI (Schemes S1 and S2). Lastly, we include the scheme S0 (WRF-Hydro) to consider WRF-Hydro calculated surface water across the land surface at 100 m-grid in the malaria modeling chain. The simulation period was set to 20 years (2000–2020) but the evaluation period span from 2015 to 2020 following the availability of the clinical data. We have carried out a suite of sensitivity experiments to calibrate relevant soil parameters in WRF-Hydro scheme S0, to produce reliable and realistic estimates of surface water in comparison to those aggregated from remote sensing data (Sentinel-1) for subsequent modeling of the malaria vector and dynamics of malaria transmission.

3.6. Ponding Water Calculations: Hydrology Comparison Method

3.6.1. Ponding Scheme S0 (WRF-Hydro)

WRF-Hydro allows estimating the instantaneous value of the depth of water ponding on the surface (units of mm).

In each grid cell, the SM (ΔSM, Equation 2) and surface water coverage (ΔPW, Equation 3) components are related by the following budget equations.

$$\Delta \mathrm{SM} = IN - EX - TR - EV - PC - SF \tag{2}$$

$$\Delta \mathrm{PW} = BP + EX - IN - OF - CF \tag{3}$$

The 1-dimensional (1D) column land surface model first computes the vertical energy fluxes (sensible and latent heat, net radiation) and moisture (canopy interception, infiltration, *infiltration-excess (IN)*, *deep percolation*, the accumulated *liquid precipitation falling on the bare soil (BP)*), as well as the thermal and moisture states of the soil. *Infiltration excess (IN)*, PW depth (PW), and SM are then disaggregated from a 1D LSM grid with a spatial resolution of 1–4 km to a high-resolution routing grid with a spatial resolution of 30–100 m using a time-step weighted method (Gochis & Chen, 2003) and passed to the *subsurface (subsurface flow (SF))* and overland flow (OF) terrain-routing modules. The key output variables, depending on the physics settings used, are the surface evaporation components (*soil evaporation (EV)*, *transpiration (TR)*, canopy water evaporation, snow sublimation, and PW evaporation). Subgrid aggregation/disaggregation is utilized in WRF-Hydro to simulate *overland (OF)* and *SF* processes at considerably finer grid resolutions than the native land surface model grid. Then, prior to routing OF, WRF-Hydro calculates subsurface lateral flow to allow *exfiltration (EX)* from fully saturated grid cells to be added to the infiltration excess computed from the LSM. *Channel flows* are cascaded upstream to downstream under the premise of negligible backwater effects.

The basic requirement for the presence of mosquitoes is the availability of water bodies. We are particularly interested in one key upgrade introduced by WRF-Hydro, which allows the IN to remain as PW. According to Bomblies et al. (2008), An. Gambiae (90% in Nouna) dispersal behaviour and Sahelian hydrologic characteristics suggest appropriate model domain dimensions of several kilometers square surrounding villages or human populations of interest and a resolution of 10 m. However, this scale may change based on the type of urbanization, road network, vegetation, water, and socio-economic level. Our choice of scale reference (100 m resolution) for mapping the potential surface water is taken from the previous studies conducted in Nouna by Dambach et al. (2009, 2012, 2018, 2019). In Nouna HDSS, Dambach et al. (2012) used remote sensing at 10 m and in-situ data for mapping surface water; they reported that the smallest pond recorded on the ground covered one 10 m pixel. Thus, direct water detection was not appropriate because object detection is feasible only when the object size is larger than the pixel size. In addition, the DEM provided useful information for mapping surface water (100 m), a higher resolution than 100 m would require significant computational, memory, and disk.

WRF-Hydro Calibration: Before implementing the experimental modeling, a series of WRF-Hydro runs in the offline mode (hydro components do not feedback to WRF) were first performed in our target region to calibrate the relevant hydrological parameters. The model calibration can be defined as finding a set of WRF-Hydro model parameters that describe temporary ponding fractions as closely as possible to the Sentinel-1. The required meteorological variables model inputs are the downward shortwave and longwave radiation, air temperature, air humidity, pressure, wind speed, and precipitation rate. WRF-Hydro is calibrated using available data from May to September for 2015, 2016, and 2017, with validation conducted from 2018 to 2020. The model optimization can involve numerous variables depending on the specific requirements or demands. Based on the literature review on flood forecasting, we identified six empirical model parameters: (a) the infiltration/runoff generation parameter (REFKDT), (b) the surface retention depth (RETDEPRTFAC), (c) the lateral saturated hydraulic conductivity (LKSATFAC), (d) the overland roughness (OVROUGHRTFAC), (e) the coefficient for deep drainage (SLOPE), and (f) the soil hydraulic parameter (Ksat) which corresponds to the scaling of saturated hydraulic conductivity. They have been documented as sensitive parameters for runoff simulation and re-infiltration process crucial for PW under different

Table 2
Experimental Design for Sensitive Model Parameters Used in This Study

Parameters	Abbreviations	Unit	Min	Max	Default	Values
Infiltration coefficient	REFKDT	–	0.1	10	3	0.1, 0.2, 0.3, 0.4, 0.5, …, 10
Surface retention depth	RETDEPRTFAC	–	0	10	1	0, 1, 2, 4, 6, 8, 10
Lateral saturated hydraulic conductivity	LKSATFAC	–	10	10,000	1,000	10, 100, 500, 1,000, 5,000, 10,000
Overland roughness	OVROUGHRTFAC	–	1	100	1	1, 2, 5, 10, 50, 100
Coefficient for deep drainage	SLOPE	–	0.1	1	0.1	0.1, 0.2, 0.5, 0.8, 1
Saturated hydraulic conductivity factor	Ksat	–				Multiply by 0.1, 0.5, 1.0, 1.5, 2.0, 2.5, 3, 3.5, 4.5, 5

hydrometeorological/geographical conditions (e.g., Arnault et al., 2016; Fersch et al., 2020; Kerandi et al., 2018; Naabil et al., 2017; Senatore et al., 2015; Silver et al., 2017; Zhang et al., 2020). Yucel et al. (2015) calibrated and validated WRF-Hydro for flood forecasting, they give an overview of the parameters and their relevance. We followed a similar approach and combined the parameters range from the previous study (Arnault et al., 2016; Zhang et al., 2020). The following steps were used for modeling: (a) We first assumed a 10 mm water depth threshold for each cell (100 m resolution) to be considered as a breeding site and (b) then compared each observed and simulated pixel to determine the number of matches/mismatches in average monthly surface water occurrence maps before and after parameters calibration. We have performed different sensitivity tests for the six parameters (see Table 2 and Supporting Information S1). Sentinel-1 and WRF-Hydro both cover a 1 km × 1 km approximate area. Sentinel-1's surface hydrology description is 10 m pixel, whereas WRF-Hydro's is 100 m. WRF-Hydro high-resolution simulations and calibrations require intensive computing resources, memory and disk. In Figure 5, we compared monthly surface water time series from simulated and Sentinel one pixel by pixel to highlight good matches (poor matches) in % for the calibration and the validation periods. After calibration, WRF-Hydro demonstrated the ability to produce the availability of potential vector breeding sites with more than 90% accuracy using Sentinel-1 data. The final parameter sets and goodness-of-fit measures are listed in Table S1 in Supporting Information S1 (Figure 6).

3.6.2. Ponding Schemes S1 and S2 (VECTRI)

Compared to WRF-Hydro, the intrinsic formulation of hydrology in the VECTRI model is highly simplified. In each cell the total water fraction, w, available for breeding is split into three categories:

$$w = w_{perm} + w_{urban} + w_{pond} \tag{4}$$

where w_{perm} is the water fraction associated with the breeding sites that are present at the borders of permanent water features such as large village ponds, lakes, or rivers (the latter is usually more commonly used by *funestus*. w_{urban} allows one to include a representation of urban-based breeding sites for vectors such as *stephensi* but is set to zero in these experiments which focus on the *gambiae* vector prevalent in the region of focus, which favors rain driven temporary ponds. These temporary ponds are represented by the term w_{pond}, which Harpex-Sahel experiments have shown that they form in regions with small-scale catchments usually limited to a few km in size (Goutorbe & Kabat, 1995; Prince et al., 1995). Two different approaches for the computation of the temporary pond w_{pond} are available in VECTRI and are explained in the following.

Scheme S1 estimates the fractional water coverage area in each time step and grid cell using a simplified surface hydrological parametrization. However, it neglects several factors, including topographical slope, lateral flow between model grid cells, soil texture (although this can now be optionally incorporated), and vegetation. The rate of change of pond fraction is given by:

$$\frac{dw_{pond}}{dt} = K_w[P(W_{\max} - W_{pond}) - W_{pond}(E + I)] \tag{5}$$

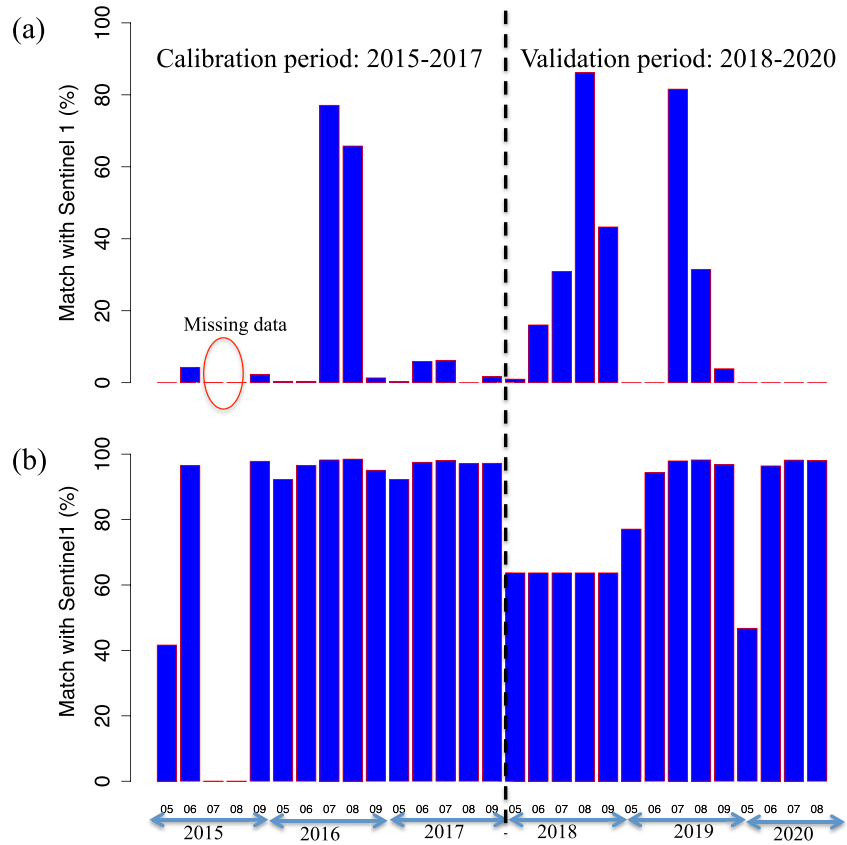

Figure 5. (a) Performance of WRF-Hydro (scheme S0) in simulating surface water during the wet months (May–September) in Nouna using the pixel match with Sentinel-1 before calibration. (b) After calibration during training (2015–2017) and validation (2018–2020) periods.

where w_{max} is the maximum temporary pond coverage area, P is precipitation rate, E and I are evaporation rate and infiltration rate respectively, and K_w is a constant that links rainfall to the growth of the temporary ponds. See the description in Tompkins and Ermert (2013) for full details on the scheme.

Scheme S2 retains the foundation of Scheme S1 but aims to rectify certain shortcomings, including deficiencies in OF, runoff, and infiltration processes. The model scheme description and configuration details are given in Asare, Tompkins, Amekudzi, et al. (2016). The relationship between the pond growth and rainfall is modified to a more

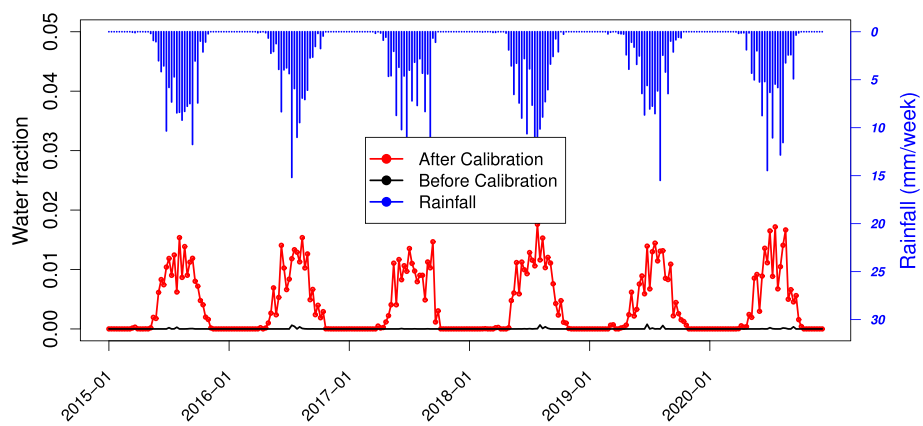

Figure 6. Simulated averaged weekly rainfall and surface water before and calibration (upper panel) in 2015–2020.

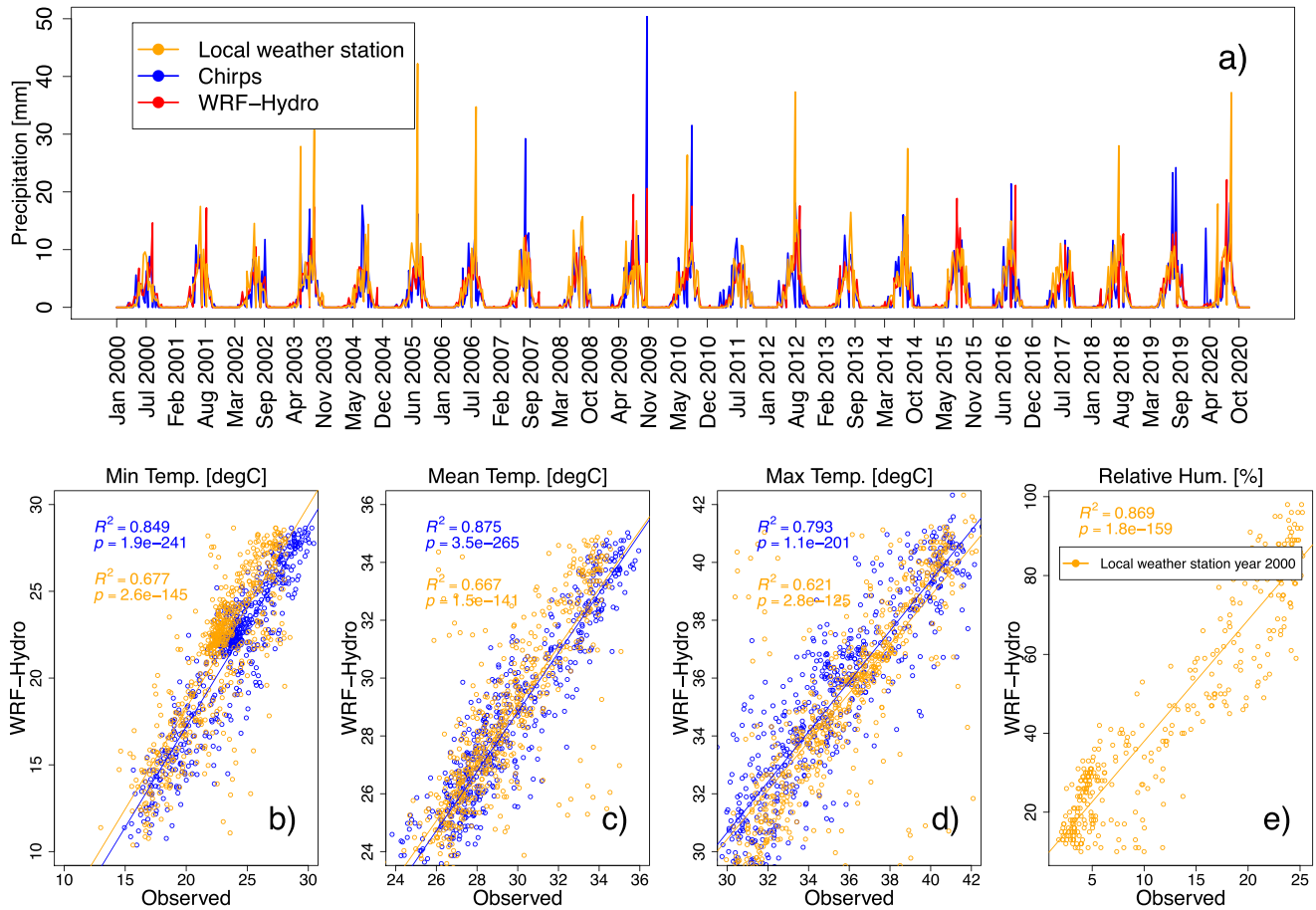

Figure 7. Nouna HDSS time series of weekly average rainfall for WRF-Hydro, CHIRPS, and observed local weather station (a) between 2000 and 2020, (b) scatter plots of simulated WRF-Hydro versus observed (CHIRTS and local weather station) for minimum temperature, (c) for mean temperature, (d) for maximum temperature for period 2000–2016, and (e) for relative humidity for 2020 only.

realistic representation of the catchment geometry, with the spatial heterogeneity of infiltration rates between the pond interior and edges accounted for. The loss of water from overflow (O), infiltration (I), and evaporation (E) are accounted for. A study done by Asare, Tompkins, Amekudzi, and Ermert (2016) over Banizoumbou village in southwestern Niger with similar climate conditions as Nouna, evaluated and showed good agreement of Scheme S2 with in situ observations.

4. Results

In the following, the climate-driven data (rainfall, temperatures, and relative humidity) from the WRF-Hydro model are first assessed against the observation data. Then, the reliability and accuracy of simulated surface water occurrence are evaluated against the observed data through Sentinel 1. Finally, we predict seasonal/interannual variability in malaria vector mosquito populations that lead to variations in malaria transmission.

4.1. Seasonal Variation of Malaria Environmental Determinants

Figure 7 compares the simulated WRF-Hydro at 1 km spatial resolution to two observed data sets (CHIRPS in blue, local weather station in orange). The weekly WRF-Hydro precipitation Figure 7a for the Nouna HDSS is relatively close to that derived from CHIRPS and local weather station, with the mean coefficient of determination (R^2) equal to 0.68 (Figure 7b). The R^2 values between WRF-Hydro and the two observed data sets (CHIRPs and local weather station) are about 0.87 and 0.69 for mean temperature (Figure 7c) and 0.79 and 0.65 for maximum temperature (Figure 7d) respectively, which indicates a good agreement between observed and

10.1029/2023WR034975

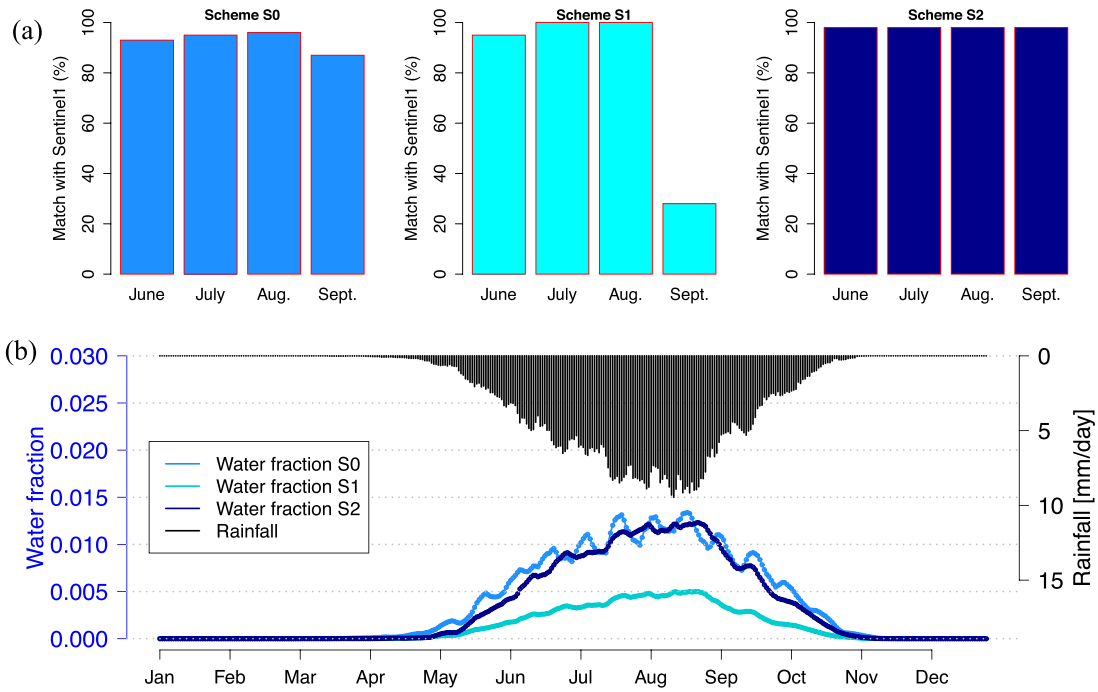

Figure 8. Comparison of average water fraction between WRF-Hydro (scheme S0), VECTRI (schemes S1 and S2) and Sentinel-1 using pixels matches (in %) during the rainy season from 2015 to 2020 (a). Weekly climatology of estimated precipitation (black line), water fraction (blue line: S0, cyan line: S1 and dark blue line: S2) (b).

simulated temperature (p-values below 0.05). The model-to-observation Root mean square error of the annual temperatures is fairly small, in the range of 0.5–1.9°C. Thus, it can be concluded that the rainfall and temperature variations are well simulated by WRF-Hydro and hence demonstrate the ability of the coupled atmosphere-hydrology modeling system to reproduce the hydrometeorological data relevant for modeling the transmission dynamics of malaria incidence in the study domain (Figures 8 and 9). Note that no bias correction is applied to climate inputs here because, in this study, model outputs from the simulation at 1 km spatial resolution were much finer than the existing observational grids. In addition, gridded observations are insufficient to correct the very high-resolution model on daily time scales, as they overestimate low-intensity precipitation due to spatial averaging (Argüeso et al., 2013).

4.2. Surface Hydrology Evaluation

Figure 8 shows the agreement between WRF-Hydro (Scheme S0), VECTRI (Schemes S1 and S2), and Sentinel-1 surface water fraction for the years 2015–2020. The S0 simulation results demonstrate the influence of calibration on water fraction estimation, WRF-Hydro could simulate water fraction fairly well, with only a 4% difference in measurements over Nouna after calibration. This finding lends credence to the hypothesis that, with knowledge of the physically based factors that affect surface hydrology, WRF-Hydro can potentially be employed to simulate the formation and persistence of the breeding habitat of mosquito vector density. The two VECTRI surface hydrology parameterization schemes (S1 and S2) can reproduce surface fractional water coverage with roughly 90% accuracy, except for S1 in September, which only matches 30% with Sentinel-1 data. It is clear from these experiments that the reason for this disparity is the different responses of the three different schemes to rainfall patterns, land use, soil type, geology, vegetation, slope, and heterogeneity in water infiltration rates. For example, 2016 (calibration period) observed wet season precipitation totaled 147 mm in June, 194 mm in July, 288 mm in August, and 78 mm in September with respectively 10 (June), 13 (July), 12 (August), and 4 (September) number of wet days with rainfall of at least 1 mm. The WRF-Hydro Scheme S0 simulation results demonstrate that the variability in the daily water fraction follows trends in rainfall relating to its maximum rainfall period, intensity, and frequency. We observed more fluctuations in S0 temporary water coverage (compared to S1 and S2) with peaks in addition to dips in June, July, August, and September. Setting the maximum infiltration parameter fix for

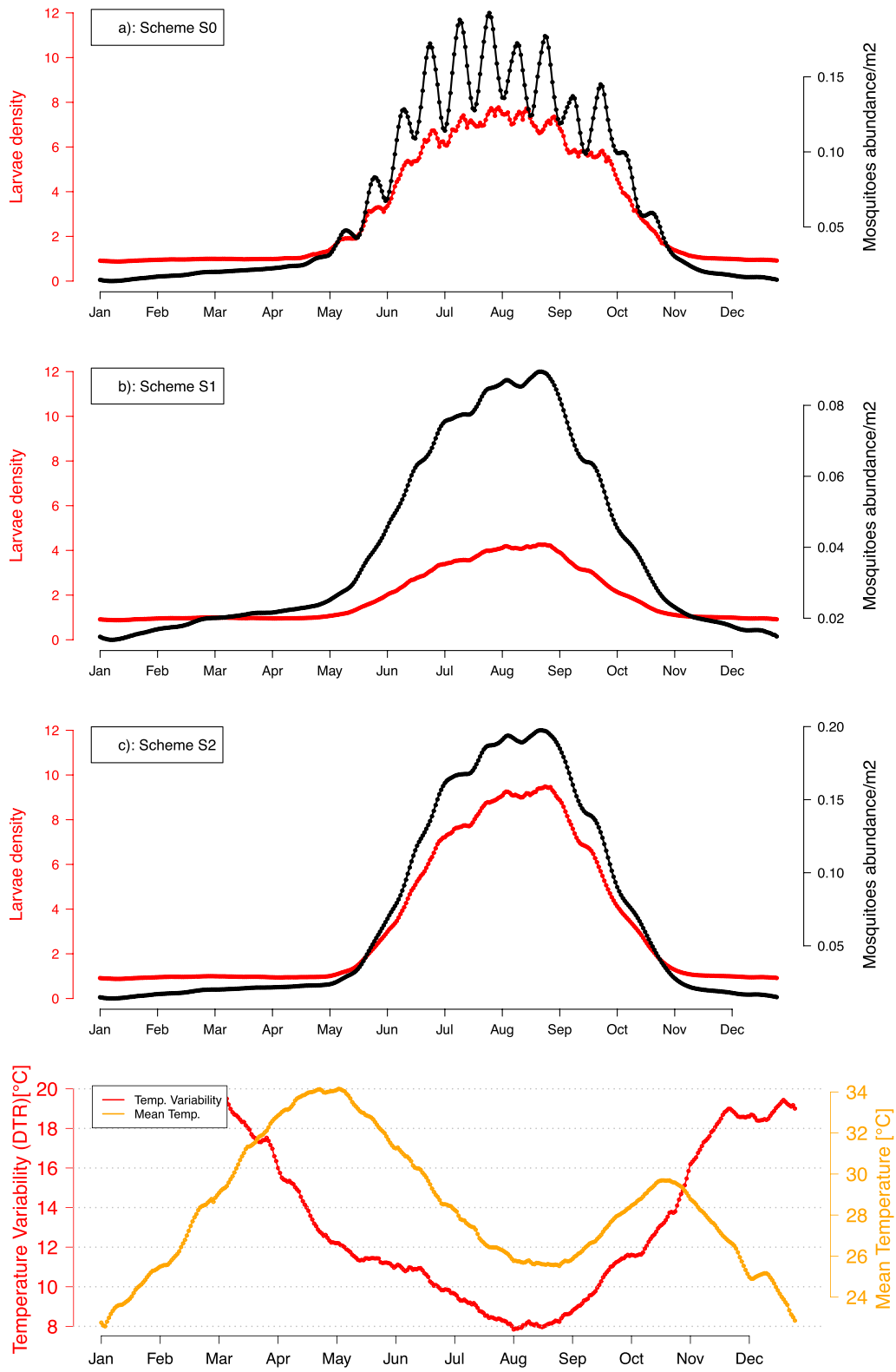

Figure 9. Time series comparison of weekly simulated larvae number (red line) and mosquitoes abundance (black line) for schemes S0 (a), S1 (b), and S2 (c) in Nouna HDSS for the period 2015–2020.

the wet season which depends on the local hydrology, soil type, and the water losses due to overflow resulted in the S2 water fraction closest to observations (Asare, Tompkins, & Bomblies, 2016). Based on previous research conducted in a Sahelian setting, approximately 90% of water loss is attributed to infiltration (Gianotti et al., 2009). S0 shows the significance of representing the infiltration process in fractional water coverage evolution, especially for areas with flat terrains and soils with high clay content like Nouna (see Figure 5 and Supporting Information S1).

4.3. Malaria Transmission Dynamics

Further, the nexus between temperatures (mean and DTR) and rainfall with water coverage, larvae number/mosquito density, and EIR in terms of weekly/monthly variations are shown in Figures 9 and 10. The EIR measures the number of infectious bites per person per unit of time. It includes the effects of vector dynamics such as mosquito development, survival, feeding activity, and parasite development.

In a month with more consecutive wet days, a significant increase in mosquito densities immediately followed (Figure 9). Both water coverage and mosquito density exhibit an upward trend beginning in July, reaching their peak in August, and later declining to negligible levels from September onward. Several water pools serving as mosquito breeding sites are mostly generated by rainfall during the rainy season. This allows mosquitoes to lay their eggs, which later develop into adult mosquitoes if the pools are sustained for at least 14 days. Our fully coupled model does keep the pools represented on the surface (Figure 8).

Seasonal temperature changes affect the larvae and mosquito seasonality, the highest larval density is recorded when the temperature variability is lower. From June to September, the mean temperature decreases (with fewer variations between the minimum and maximum), while the mosquito abundance per km^2 increases with rainfall and temperature (when temperatures range between 26 and 29°C and rainfall exceeds 10 mm/day). With temperatures exceeding 30°C and rainfall below 3 mm/day, the vector density decrease reaches its minimum. Indeed, Anopheles develops from a juvenile to an adult stage under optimum conditions of 28°C in around 14 days, whereas falciparum malaria symptoms appear between 7 and 15 days later depending on the host's immunity (Depinay et al., 2004; Ermert et al., 2011; Laneri et al., 2010). In VECTRI-simulated Scheme S1, the water coverage and the mosquito density start just after the first recorded amount of rainfall, while with VECTRI-simulated Scheme S2 the mosquito density starts one to 2 weeks later. The density of larvae or mosquitoes with S0 closely resembles that with S2. Most noticeable here is VECTRI model response to hydrological inputs, particularly between the conceptual model (S1 and S2) and detailed physical processes model (S0).

We find that mosquitoes had their highest abundance in August with high biting activity of up to 20 bites per person per day (Figures 10f–10h and 10j) and contrast with research findings of Dambach et al. (2018) in Nouna HDSS. Dambach et al. (2018) conducted a negative binomial regression framework to statistically analyze the host-seeking activities of Anopheles species across hours, months, and villages. They observed differences in the pattern of biting cycles between the early peak (around 25 bites) and late rainy season (10 bites). The findings here again confirm a significant association between a rise in malaria risk in a given month and an increase in the total accumulated rainfall (rainfall is high in the province Figures 10 and 11) during that month and the 2–3 months preceding it. There were only minor rainfalls after End-October, Anopheles activity stayed above 5 bites per person per day until the end of the rainy season.

The monthly malaria incidence from 2015 to 2020 is shown in Figure 11, the model results are displayed as a set of statistics showing the standardized anomalies of the predictive model against real outcomes from the data (lower panel). In terms of month-wise malaria cases, it becomes clear from Figure 11 (upper panel) that the VECTRI model is sensitive to surface hydrology representation for the predicted number of cases. The overall picture of VECTRI-simulated seasonal malaria variability (lower panel) is similar to those reported. However, it's worth noting a delay ranging from 2 weeks (VECTRI-S0) to 1 month (VECTRI-S1 and S2) before the observed onset of the malaria season. Our study reveals that by leveraging knowledge of the direct interaction between hydroclimatological processes and climate variability on malaria risk, we can accurately simulate malaria dynamics using a dynamical malaria transmission model system.

10.1029/2023WR034975

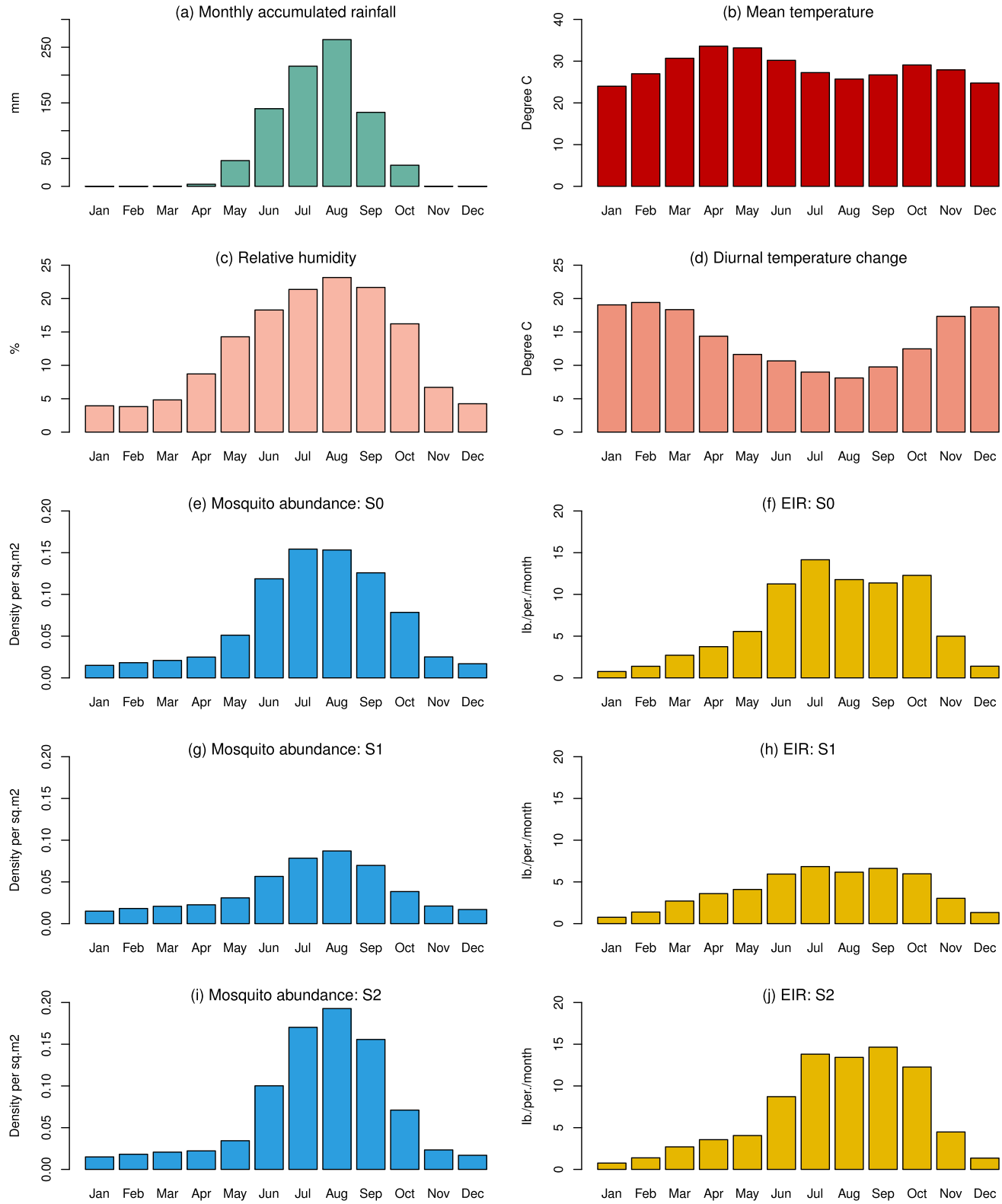

Figure 10. Monthly variation of simulated climate ((a)–(d): rainfall, mean temperature, relative humidity, diurnal temperature range) and malaria parameters ((e)–(j): mosquito density and EIR) from 2015 to 2020. Only the latter two parameters depend on the applied scheme, that is, WRF-Hydro scheme S0, VECTRI-simulated schemes (S1 and S2).

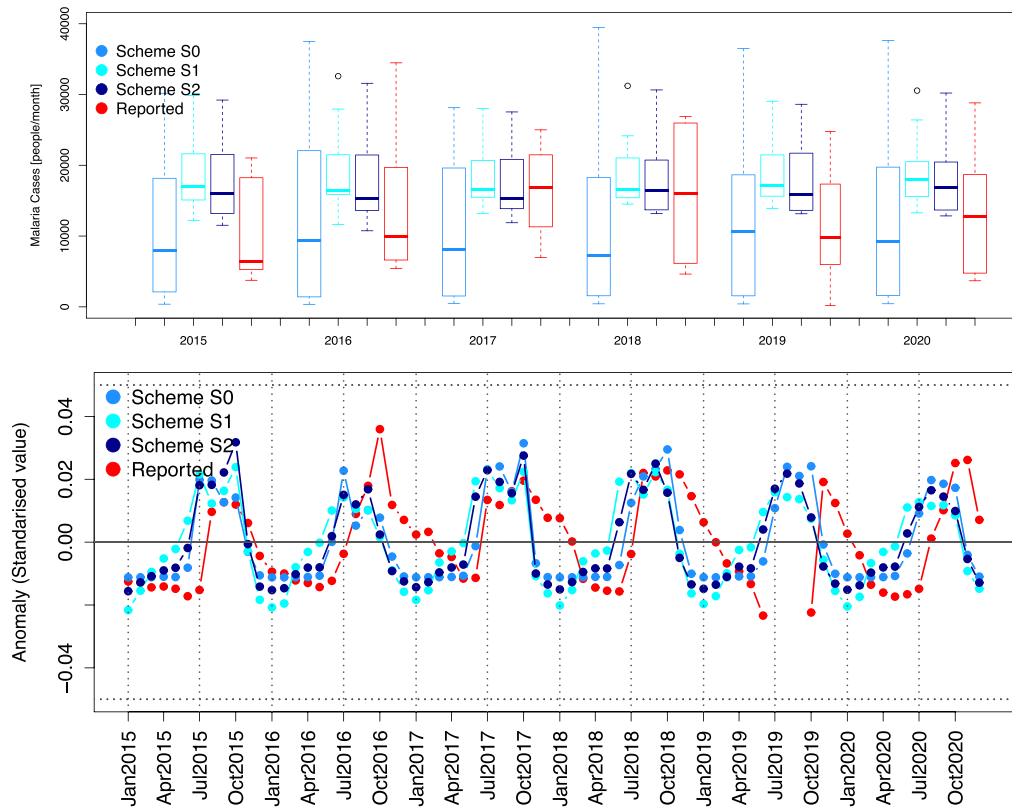

Figure 11. Boxplot of the annual malaria cases (upper panel). Values represent, from top to bottom, maximum, median, and minimum. The low panel illustrates the seasonal transmission periods of monthly malaria cases across Nouna HDSS from 2015 to 2020 of observed cohort malaria data compared to simulated scheme S0, S1, and S2 anomalies.

5. Discussion

The transmission force of malaria infection requires the interaction of environmental risk factors jointly with the human host, the malaria parasite, and the Anopheles vector. Temperature, precipitation, and humidity are examples of environmental risk factors. However, another crucial environmental risk factor affecting malaria transmission is the availability of temporary PW, essential for the vector mosquito larval habitats and development (e.g., Bomblies et al., 2008; Getachew et al., 2020; Mwakalinga et al., 2018; Smith et al., 2013; Yamana et al., 2016). The crucial points of our study are to investigate the sensitivity/performance of three different surface hydrological approaches, aiming to quantitatively estimate the malaria vector larval habitats (i.e., the PW) in combination with other climatic variables. The idea is to implement the physical processes involved in the hydro-climatic malaria transmission chain, following the study of Smith et al. (2020) in which the Lisflood hydrological model (Van Der Knijff et al., 2010) was coupled with a malaria climate suitability model for Africa. The authors highlighted the importance of moving forward to fine-scale hydrological processes: (a) to determine the availability of Anopheles breeding habitat, (b) to permit other physical processes, such as the larval flushing effects of high-velocity river flows, and (c) to depict vector habitats explicitly. In this contribution, our first method (Scheme S0) is based on a coupled atmospheric- and terrestrial model system, with 1 km grid spacing for the atmospheric and 100 m grid spacing for the hydrological part. The second method (Scheme S1) is derived from simple (implicit) surface hydrological simulations (rainfall drives the puddle model). The third method (Scheme S2) builds upon the concept of Scheme S1, incorporating additional detailed information regarding soil texture and considering variables such as infiltration. Unlike Scheme S1, the evaporation rate in Scheme S2 is not held constant. On the one side, depending on the hydrological used schemes, the model system consisting of WRF-Hydro and VECTRI can provide results comparable to previous malaria transmission studies. On the other side, it documents the necessity of further efforts to build this capability. The performance of our joint hydro-climate-malaria modeling is discussed in the following.

5.1. Joint WRF-Hydro VECTRI Model Results and Its Limitations

We stress three points that explain the variation in results for the specific case in the Nouna HDSS area: (a) the climate-driven variability, (b) the prediction of PW, and (c) the malaria transmission intensity.

5.1.1. Climate-Driven Variability

The WRF-Hydro model outputs reflected the observed in-situ climate data (rainfall, mean-, minimum-, and maximum temperatures, as well as diurnal temperature range) reasonably well with minor exceptions (e.g., high correlation coefficients with p-values below 0.05). This proves the ability of the coupled atmosphere-hydrology modeling system to reproduce the hydrometeorological data consistent with findings from previous studies (Naabil et al., 2017; Quenum et al., 2022; Z. Zhang et al., 2021). Our simulations revealed at least 40%–60% (Figure 5 and Figure S3 in Supporting Information S1) of the research area might have served as a potential larval habitat (temporary water coverage). Dambach et al. (2009) observed in Nouna up to 60% of the surface within the 500 m buffer covered with very high and high-risk habitats. Our results are in line with the previous malaria studies that related the amount and sub-seasonal variability of rainfall to the increase of mosquito density through the availability of anopheline mosquito breeding sites (Bomblies, 2012; Bomblies et al., 2008). Mosquito density values decrease above a certain threshold (temperature above 30°C and rainfall less than 3 mm/day). Further, modeling revealed that both minimum and maximum temperature ranges significantly affect the development of the malaria parasite and its mosquito vector. Numerous research from tropical and semi-tropical regions of the world (Blanford et al., 2013; Mohammadkhani et al., 2016; Ouedraogo et al., 2018) studied the relationship between temperature and malaria, and the findings are consistent with our study.

5.1.2. Prediction of Ponded Water

Regarding the surface hydrology scheme efficiencies, we can conclude that the WRF-Hydro surface hydrology scheme (S0) accurately reproduces the seasonal and intraseasonal changes in the surface water fraction (Figure 5) ranging from 20% before calibration to 96% after calibration when compared to Sentinel-1 data at 100-m resolution. The advantage of WRF-Hydro compared with the existing S1 and S2 is that it improves the description of lateral terrestrial water movement, which is not expressed in these standard models. According to earlier studies, with the use of an appropriate calibration method, WRF-hydro can simulate SM, estimate streamflow, and identify associated flood events (Arnault et al., 2016; Givati et al., 2011; Yucel et al., 2015). We find the effects of the different tested parameters on the spatio-temporal evolution of fractional water coverage (Figure S2 in Supporting Information S1). Meng et al. (2023) compared the performance of the developed lateral terrestrial water schemes flow in Noah-MP to improve SM representation. The findings show that maximum infiltration has a considerable influence on volumetric SM, which in turn influences the depth of water inundation (Figures 8 and 9 and Figures S3 and S4 in Supporting Information S1). Suppose the soil infiltration rate is faster after the rain, it minimizes any standing water, which in turn shortens the lifespan of mosquitoes to the extent that malaria transmission does not occur. Following calibration, the model accurately reproduces the impact of rainfall variability on simulated daily pond fraction (see Figure 4), facilitating the methodology's application across different regions. For the cases studied here, it has been determined that in addition to rainfall, these three parameters (saturated hydraulic conductivity (Ksat), runoff partition parameter (REFKDT), and the overland roughness (OVROUGHRTFAC)) have the most substantial impacts on the water fraction estimation process (Figure S2 in Supporting Information S1). Those model parameters are surface runoff scaling parameters used in the Noah-MP model to limit the amount of runoff produced for a given volume of precipitation. This implies that alterations or fluctuations in these parameters may exert a comparatively stronger influence on the predicted levels of PW compared to other parameters examined. Givati et al. (2016) performed WRF-Hydro model simulations to determine the potential added value for hydrometeorological predictions and flood forecasting, they documented that REFKDT can significantly influence surface infiltration and partition of total runoff into surface and subsurface runoff, where increasing REFKDT leads to a decrease in surface runoff (Niu et al., 2011). As found in this study, the sensitivity of the infiltration processes to these three parameters was confirmed in the results of Zhang et al. (2020). The fully coupled modeling approach potentially yields even more significant improvements when complemented by timely and accurate maps of observed surface water (Remote sensing plus in situ data). Accessing such information can be beneficial for mapping malaria risk and targeting disease control interventions effectively. However, other studies recommended that current product methods may not be suitable

for effectively mapping dynamic and frequently obscured aquatic habitats of mosquitoes, especially those concealed by emergent vegetation (Hardy et al., 2019).

5.1.3. Malaria Transmission Intensity

We found that VECTRI is a suitable model for investigating malaria transmission with a stronger ability to capture the levels of malaria endemicity. Our results prove that VECTRI model is sensitive to surface hydrology representation for larvae density, vector abundance and EIR variables. The simulated malaria incidence range is in agreement with the signs of the observations change (peak of malaria e.g. from June to September and the decreasing malaria cases on time). Studies by Asare and Amekudzi (2017) in Ghana and Fall et al. (2022) in Senegal using VECTRI yielded similar results. However, the current model tuning does not consider the introduction of various vector control interventions (such as bednet use), leading to an earlier onset of malaria season as shown in Figure 11. The decline in both clinical episodes and deaths due to malaria is primarily associated with the expansion of vector-control measures, such as insecticide-treated bednets and indoor residual spraying (Elmardi et al., 2021; Musiime et al., 2019; Sadoine et al., 2024). While tuning model parameters, we observed a significant sensitivity of VECTRI schemes S1 and S2 to the parameter "wperm" (fraction of permanent water bodies, see Equation 4), that is, setting "wperm" to 0.001 produces results that match the observed malaria cases from January to May. This indicates that the parameter "wperm" plays a crucial role in influencing the model's performance or predictions during this time frame. This might be a structural error in the model that requires further attention beyond parameter adjustments. Further, certain modifications and improvements are required in VECTRI. One potential solution could involve adjusting the permanent fraction to only impact a small fraction nearby instead of the whole domain. On the other hand, the study proves that the VECTRI model effectively reproduces the seasonal cycle of malaria cases in response to the rainy season, as highlighted by Tompkins and Thomson (2018). Additional research on parameters contributing most to VECTRI output variability is required to strengthen the knowledge base to reduce VECTRI output uncertainty, for example, as discussed by Parihar et al. (2024). In 2021, the African Region was home to 95% of malaria cases and 96% of malaria deaths. Approximately 80% of all malaria-related deaths in the region were among children under 5 years old (WHO, 2023). An important future development of the VECTRI representation of malaria transmission is age-specific to supply much information about the force of infection and malaria burden in the population. Future research should explore environmental changes, socioeconomic status, human activities such as farming, and population movement and settlement (density) in the VECTRI model.

5.2. Uncertainty Around Reported Malaria Cases

As stated above, additional uncertainties arise from the reported cases (gaps between the healthcare facilities and government statistics). This is attributed to a high bias and obscurity rate, particularly in SSA, due to out-of-sample generalization over space and time, erroneous diagnosis, and under-counting due to varying health-seeking behaviour and policy (e.g., Yamba et al. (2022)). Our major limitation in Nouna was the inability to distinguish between true missing values and "no data reported" as the case from July–October 2019, when personnel from the health sector were on strike (Sangaré et al., 2022), see Figure 11. Uncertainty in malaria case estimates in SSA ranges from approximately 30%–50% of the total numbers reported in the high-prevalence SSA countries (Sullivan, 2010). The WHO Global Technical Strategy for Malaria aims to achieve a reduction of 90% in both case incidence and malaria deaths by 2030 compared to the levels recorded in 2015. We have learned that malaria is declining across SSA, from millions to about half a million deaths a year in 2018 (WHO, 2018). Despite these advances, persistent uncertainties are observed in the highest malaria burden regions and those expected to experience the highest decline (e.g., Nkumama et al., 2017). These targets as well as the need for capital investment, and good knowledge about all malaria-determining factors and methodologies require accurate surveillance to lower the limited availability of high-quality data that is up to date and will offer benefits for climate change studies.

6. Conclusions and Future Prospects

The findings underscore the importance of specific hydrological input variables, particularly surface water, and their interaction with climate factors in shaping the spread of malaria-carrying mosquitoes. We highlight the differences between conceptual and detailed physical process models in malaria hydrology. The calibration of the WRF-Hydro model at 100 m using field data was comparable to hydrological and entomological conditions using

the VECTRI model. The WRF-Hydro and VECTRI model coupling effectively depicts distributed hydrology that fosters suitable breeding habitats for Anopheles mosquitoes, accurately capturing observed population dynamics across seasonal and interannual scales. Nonetheless, the analysis is subject to uncertainties stemming from various sources, including the multitude of model parameters in both VECTRI and WRF-Hydro. These parameters contribute to the complexity of the models and introduce uncertainties in the simulation outcomes. Additionally, data limitations pose significant challenges, particularly concerning the availability of comprehensive data sets for validation purposes (short time series about malaria incidences, the high number of unreported cases, and missing data for validation of PW). The model's performance could further be improved through (a) enhancing the quality and quantity of epidemiological data (such as case numbers/EIR and vector control interventions) gathered from extensive and prolonged surveys or programs, and (b) refining the modeling system by (a) increasing the resolution of WRF-Hydro beyond 100 m for better representation of water bodies, and (b) integrating sensitivity analyses of VECTRI model input parameters to gain deeper understanding on their impacts on the state variables, particularly concerning malaria disease transmission and prevalence.

Data Availability Statement

The 1 km WRF and WRF-Hydro simulations (Dieng et al. (2024)) are available at Zenodo store via https://doi.org/10.5281/zenodo.10868443. Technical information about HydroSHEDS data is available online at https://www.hydrosheds.org/hydrosheds-core-downloads. The WRF-Hydro preprocessing tool is available online at https://ral.ucar.edu/projects/wrf_hydro/pre-processing-tools. The Malaria data used in this study are available from the Centre de Recherche en Santé de Nouna (CRSN)'s Institutional Data Access/Ethics Committee for researchers who meet the criteria for access to confidential data. The HDSS data can be accessed by contacting sieali@yahoo.fr. Satellite-based Sentinel-1 data information and access can be found at https://sentinel.esa.int/web/sentinel/sentinel-data-access.

The weather station data can be obtained by contacting the Burkina-Faso National Meteorological Agency (https://www.meteoburkina.bf/). Climate Hazards Group InfraRed Precipitation with Station data (CHIRPS, Funk et al. (2015)) information and data access can be obtained at https://www.chc.ucsb.edu/data/chirps. The minimum and maximum CHIRTS-daily temperatures can be downloaded from https://data.chc.ucsb.edu/products/CHIRTSdaily/v1.0/ (Funk et al., 2019). The gridded population density data sets can be accessed from https://sedac.ciesin.columbia.edu/data/set/gpw-v4-population-density-rev11 (Doxsey-Whitfield et al., 2015).

Acknowledgments

The study has been conducted within the broader framework of the research project *German Research Foundation* (DFG) through the *FOR 2936: Climate Change and Health in Sub-Saharan Africa* project (Grant KU2090/14-1). The authors thank the Steinbuch Centre for Computing for providing access to the Horeka supercomputer and the Karlsruhe Institute of Technology/IMK-IFU for providing computing resources at the Linux cluster. We thank the Remote Sensing Solutions GmbH (RSS) for providing data. We also acknowledge the kind support of the International Centre for Theoretical Physics. We want to thank the meteorological services of Burkina Faso and the Centre de Recherche en Santé de Nouna (CRSN) for providing the daily weather and malaria data sets.

References

Abiodun, G., Maharaj, R., Witbooi, P., & Okosun, K. (2016). Modelling the influence of temperature and rainfall on the population dynamics of anopheles arabiensis. *Malaria Journal*, *15*(1), 364. https://doi.org/10.1186/s12936-016-1411-6

Abiodun, G., Witbooi, P., & Okosun, K. (2017). Modeling and analyzing the impact of temperature and rainfall on mosquito population dynamics over Kwazulu-Natal, South Africa. *International Journal of Biomathematics*, *10*(04), 1750055. https://doi.org/10.1142/S1793524517500553

Abiodun, G., Witbooi, P., & Okosun, K. (2018). Modelling the impact of climatic variables on malaria transmission. *Hacettepe Journal of Mathematics and Statistics*, *47*(2), 219–235.

Argüeso, D., Evans, J., & Fita, L. (2013). Precipitation bias correction of very high resolution regional climate models. *Hydrology and Earth System Sciences*, *17*(11), 4379–4388. https://doi.org/10.5194/hess-17-4379-2013

Arnault, J., Fersch, B., Rummler, T., Zhang, G. Z., Wei, J. G., Wei, J., et al. (2021). Lateral terrestrial water flow contribution to summer precipitation at continental scale – A comparison between Europe and West Africa with WRF-Hydro-tag ensembles. *Hydrological Processes*, *35*(5), e14183. https://doi.org/10.1002/hyp.14183

Arnault, J., Wagner, S., Rummler, T., Fersch, B., Bliefernicht, J., Andresen, S., & Kunstmann, H. (2016). Role of runoff-infiltration partitioning and resolved overland flow on land-atmosphere feedbacks: A case study with the WRF0-Hydro coupled modeling system for West Africa. *Journal of Hydrometeorology*, *17*(5), 1489–1516. https://doi.org/10.1175/JHM-D-15-0089.1

Asare, E. O., & Amekudzi, L. K. (2017). Assessing climate driven malaria variability in Ghana using a regional scale dynamical model. *Climate*, *5*(1), 20. https://doi.org/10.3390/cli5010020

Asare, E. O., Tompkins, A., Amekudzi, L., & Ermert, V. (2016). A breeding site model for regional, dynamical malaria simulations evaluated using in situ temporary ponds observations. *Geospatial health*, *11*(s1), 390. https://doi.org/10.4081/gh.2016.390

Asare, E. O., Tompkins, A., Amekudzi, L., Ermert, V., & Redl, R. (2016). Mosquito breeding site water temperature observations and simulations towards improved vector-borne disease models for Africa. *Geospatial health*, *11*(s1). https://doi.org/10.4081/gh.2016.391

Asare, E. O., Tompkins, A. M., & Bomblies, A. (2016). A regional model for malaria vector developmental habitats evaluated using explicit, pond-resolving surface hydrology simulations. *PLoS One*, *11*(3), e0150626. https://doi.org/10.1371/journal.pone.0150626

Ayanlade, A., Sergi, C. M., Sakdapolrak, P., Ayanlade, O. S., Di Carlo, P., Babatimehin, O. I., et al. (2022). Climate change engenders a better Early Warning System development across Sub-Saharan Africa: The malaria case. *Resources, Environment and Sustainability*, *10*, 100080. https://doi.org/10.1016/j.resenv.2022.100080

Badmos, A., Alaran, A., Adebisi, Y., Bouaddi, O., Onibon, Z., Dada, A., et al. (2021). What Sub-Saharan African countries can learn from malaria elimination in China. *Tropical Medicine and Health*, *49*(1), 86. https://doi.org/10.1186/s41182-021-00379-z

Blanford, J., Blanford, S., Crane, R., Mann, M., Paaijmans, K., Schreiber, K., & Thomas, M. (2013). Implications of temperature variation for malaria parasite development across Africa. *Scientific Reports*, *3*(1), 1300. https://doi.org/10.1038/srep01300

Bomblies, A. (2012). Modeling the role of rainfall patterns in seastransmission transmission. *Climatic Change*, *112*(3), 673–685. https://doi.org/10.1007/s10584-011-0230-6

Bomblies, A., Duchemin, J., & Eltahir, E. (2008). Hydrology of malaria: Model development and application to a Sahelian village. *Water Resources Research*, *44*(12). https://doi.org/10.1029/2008WR006917

Caminade, C., Kovats, S., Rocklov, J., Tompkins, A., Morse, A., Colón-González, F., et al. (2014). Impact of climate change on global malaria distribution. *Proceedings of the National Academy of Sciences of the United States of America*, *111*(9), 3286–3291. https://doi.org/10.1073/pnas.1302089111

Campbell, P., Bash, J., & Spero, T. (2019). Updates to the Noah land surface model in WRF-CMAQ to improve simulated meteorology, air quality, and deposition. *Journal of Advances in Modeling Earth Systems*, *11*(1), 231–256. https://doi.org/10.1029/2018MS001422

Christiansen-Jucht, C., Parham, P., Saddler, A., Koella, J., & Basáñez, M. (2015). Larval and adult environmental temperatures influence the adult reproductive traits of *Anopheles gambiae* ss. *Parasites & Vectors*, *8*(456), 456. https://doi.org/10.1186/s13071-015-1053-5

Colón-González, F., Sewe, M., Tompkins, A., Sjödin, H., Casallas, A., Rocklöv, J., et al. (2021). Projecting the risk of mosquito-borne diseases in a warmer and more populated world: A multi-model, multi-scenario intercomparison modelling study. *The Lancet Planetary Health*, *5*(7), e404–e414. https://doi.org/10.1016/S2542-5196(21)00132-7

Constantinidou, K., Hadjinicolaou, P., Zittis, G., & Lelieveld, J. (2020). Performance of land surface schemes in the WRF model for climate simulations over the MENA-CORDEX domain. *Earth Systems and Environment*, *4*(4), 647–665. https://doi.org/10.1007/s41748-020-00187-1

Dambach, P., Jorge, M. M., Traore, I., Phalkey, R., Sawadogo, H., Zabre, P., et al. (2018). A qualitative study of community perception and acceptance of biological larviciding for malaria mosquito control in rural Burkina Faso. *BMC Public Health*, *18*(1), 399. https://doi.org/10.1186/s12889-018-5299-7

Dambach, P., Machault, V., Lacaux, J.-P., Vignolles, C., Sie, A., & Sauerborn, R. (2012). Utilization of combined remote sensing techniques to detect environmental variables influencing malaria vector densities in rural West Africa. *International Journal of Health Geographics*, *11*(1), 8. https://doi.org/10.1186/1476-072X-11-8

Dambach, P., Schleicher, M., Korir, P., Ouedraogo, S., Dambach, J., Sie, A., et al. (2019). Nightly biting cycles of anopheles species in rural northwestern Burkina Faso. *Journal of Medical Entomology*, *55*(4), 1027–1034. https://doi.org/10.1093/jme/tjy043

Dambach, P., Si, A., Lacaux, J., Vignolles, C., Machault, V., & Sauerborn, R. (2009). Using high spatial resolution remote sensing for risk mapping of malaria occurrence in the Nouna district, Burkina Faso. *Global Health Action*, *2*(1), 2094. https://doi.org/10.3402/gha.v2i0.2094

Depinay, J., Mbogo, C., Killeen, G., Knols, B., Beier, J., Carlson, J., et al. (2004). A simulation model of African Anopheles ecology and population dynamics for the analysis of malaria transmission. *Malaria Journal*, *3*(1), 29. https://doi.org/10.1186/1475-2875-3-29

Desconnets, J., Vieux, B., Cappelaere, B., & Delclaux, F. (1996). A GIS for hydrological modeling in the semiarid, HAPEX-Sahel experiment area of Niger, Africa. *Transactions in GIS*, *1*(2), 82–94. https://doi.org/10.1111/j.1467-9671.1996.tb00036.x

Diaz, J., González, A., Expósito, F., Pérez, J., Fernández, J., Garc'ıa-Díez, M., & Taima, D. (2015). WRF multi-physics simulation of clouds in the African region. *Quarterly Journal of the Royal Meteorological Society*, *141*(692), 2737–2749. https://doi.org/10.1002/qj.2560

Diboulo, E., Sié, A., & Vounatsou, P. (2016). Assessing the effects of malaria interventions on the geographical distribution of parasitaemia risk in Burkina Faso. *Malaria Journal*, *15*(1), 228. https://doi.org/10.1186/s12936-016-1282-x

Dieng, M. D. B., Adrian, M. T., Joel, A., Ali, S., Benjamin, F., Patrick, L., et al. (2024). 1-km high resolution model outputs using the WRF and WRF-Hydro model raw data from the manuscript "Process-based Atmosphere-Hydrology-Malaria Modeling: Performance for Spatio-temporal Malaria Transmission Dynamics in Sub-Saharan Africa" [Dataset]. *Water Resources Research*. https://doi.org/10.5281/zenodo.10868443

Diouf, I., Adeola, A., Abiodun, G., Lennard, C., Shirinde, J., Yaka, P., et al. (2020). Impact of future climate change on malaria in West Africa. *Theoretical and Applied Climatology*, *147*(3), 853–865. https://doi.org/10.1007/s00704-021-03807-6

Doxsey-Whitfield, E., MacManus, K., Adamo, S. B., Pistolesi, L., Squires, J., Borkovska, O., & Baptista, S. R. (2015). Taking advantage of the improved availability of census data: A first look at the gridded population of the world, version 4 [Dataset]. *Papers in Applied Geography*, *1*(3), 226–234. https://doi.org/10.1080/23754931.2015.1014272

Dudhia, J. (1989). Numerical study of convection observed during the winter monsoon experiment using a mesoscale two-dimensional model. *Journal of the Atmospheric Sciences*, *46*(20), 3077–3107. https://doi.org/10.1175/1520-0469(1989)046<3077:nsocod>2.0.co;2

Ek, M., Mitchell, K., Lin, Y., Rogers, E., Grunmann, P., Koren, V., et al. (2003). Implementation of Noah land surface model advances in the National Centers for Environmental Prediction operational mesoscale Eta model. *Journal of Geophysical Research*, *108*(D22), 8851. https://doi.org/10.1029/2002JD003296

Elmardi, K. A., Adam, I., Malik, E. M., Kafy, H. T., Abdin, M. S., Kleinschmidt, I., & Kremers, S. (2021). Impact of malaria control interventions on malaria infection and anaemia in areas with irrigated schemes: A cross-sectional population-based study in Sudan. *BMC Infectious Diseases*, *21*(1), 1248. https://doi.org/10.1186/s12879-021-06929-4

Ermert, V., Fink, A., Jones, A., & Morse, A. (2011). Development of a new version of the Liverpool Malaria Model. I. Refining the parameter settings and mathematical formulation of basic processes based on a literature review. *Malaria Journal*, *10*(1), 35. https://doi.org/10.1186/1475-2875-10-35

Fall, P., Diouf, I., Deme, A., & Sene, D. (2022). Assessment of climate-driven variations in malaria transmission in Senegal using the VECTRI model. *Atmosphere*, *13*(3), 418. https://doi.org/10.3390/atmos13030418

Fersch, B., Senatore, A., Adler, B., Arnault, J., Mauder, M., Schneider, K., et al. (2020). High-resolution fully coupled atmospheric-hydrological modeling: A cross-compartment regional water and energy cycle evaluation. *Hydrology and Earth System Sciences*, *24*(5), 2457–2481. https://doi.org/10.5194/hess-24-2457-2020

Funk, C., Peterson, P., Landsfeld, M., Pedreros, D., Verdin, J., Rowland, J., et al. (2014). A quasi-global precipitation time series for drought monitoring. *U.S. Geological Survey*, *832*, 4. https://doi.org/10.3133/ds832

Funk, C., Peterson, P., Landsfeld, M., Pedreros, D., Verdin, J., Shukla, S., et al. (2015). The climate hazards infrared precipitation with stationsÑa new environmental record for monitoring extremes [Dataset]. *Scientific Data*, *2*(1), 150066. https://doi.org/10.1038/sdata.2015.66

Funk, C., Peterson, P., Peterson, S., Shukla, S., Davenport, F., Michaelsen, J., et al. (2019). A high-resolution 1983–2016 t_{max} climate data record based on infrared temperatures and stations by the climate hazard center [Dataset]. *Journal of Climate*, *32*(17), 5639–5658. https://doi.org/10.1175/JCLI-D-18-0698.1

Gallant, J. C., & Dowling, T. I. (2003). A multiresolution index of valley bottom flatness for mapping depositional areas. *Water Resources Research*, *39*(12). https://doi.org/10.1029/2002WR001426

García-Ortega, E., Achugbu, I., Dudhia, J., Olufayo, A., Balogun, I., Adefisan, E., & Gbode, I. (2020). Assessment of WRF land surface model performance over West Africa. *Advances in Meteorology*, *2020*(6205308), 1–30. https://doi.org/10.1155/2020/6205308

Getachew, D., Balkew, M., & Tekie, H. (2020). Anopheles larval species composition and characterization of breeding habitats in two localities in the Ghibe River Basin, southwestern Ethiopia. *Malaria Journal*, *19*(1), 65. https://doi.org/10.1186/s12936-020-3145-8
Gianotti, R. L., Bomblies, A., & Eltahir, E. A. B. (2009). Hydrologic modeling to screen potential environmental management methods for malaria vector control in Niger. *Water Resources Research*, *45*(8). https://doi.org/10.1029/2008WR007567
Gilles, H. (1993). Epidemiology of malaria. In H. M. Gilles & D. A. Warrel (Eds.), *Bruce-Chwatt's essential malariology* (pp. 124–163.55). EdwardArnold.
Givati, A., Gochis, D., Rummler, T., & Kunstmann, H. (2016). Comparing one-way and two-way coupled hydrometeorological forecasting systems for flood forecasting in the Mediterranean region. *Hydrology*, *3*(2), 19. https://doi.org/10.3390/hydrology3020019
Givati, A., Lynn, B., Liu, Y., & Rimmer, A. (2011). Using the WRF model in an operational streamflow forecast system for the Jordan River. *Journal of Applied Meteorology and Climatology*, *51*(2), 285–299. https://doi.org/10.1175/JAMC-D-11-082.1
Gochis, D. J., Barlage, M., Dugger, A., FitzGerald, K., Karsten, L., McAllister, M., et al. (2018). *The WRF-Hydro modeling system technical description (Version 5.0)*. NCAR Tech. Note, 107. Retrieved from https://ral.ucar.edu/sites/default/files/public/WRF-HydroV5TechnicalDescription.pdf
Gochis, D. J., & Chen, F. (2003). *Hydrological enhancements to the community Noah land surface model: Technical description* (NCAR Sci. Tech. Note TN-454+STR, p. 68). National Center for Atmospheric Research (NCAR). Retrieved from https://nldr.library.ucar.edu/repository/assets/technotes/TECH-NOTE-000-000-000-516.pdf
Goutorbe, J., & Kabat, P. (1995). Global change: Climate change and climate change impacts; focusing of European research (pp. 661–694).
Gridded population of the world. (2018). *Gridded population of the world, version 4 (GPWv4): Population density, revision 11*. NASA Socioeconomic Data and Applications Center (SEDAC). https://doi.org/10.7927/H49C6VHW
Hardy, A., Ettritch, G., Cross, D., Bunting, P., Liywalii, F., Sakala, J., et al. (2019). Automatic detection of open and vegetated water bodies using Sentinel 1 to map African malaria vector mosquito breeding habitats. *Remote Sensing*, *11*(5), 93. https://doi.org/10.3390/rs11050593
Heinzeller, D., Dieng, D., Smiatek, G., Olusegun, C., Klein, C., Hamann, I., et al. (2018). The WASCAL high-resolution regional climate simulation ensemble for West Africa: Concept, dissemination and assessment. *Earth System Science Data*, *10*(2), 815–835. https://doi.org/10.5194/essd-10-815-2018
Hersbach, H., Bell, B., Berrisford, P., Hirahara, S., Horányi, A., Muñoz-Sabater, J., et al. (2020). The ERA5 global reanalysis. *Quarterly Journal of the Royal Meteorological Society*, *146*(730), 1999–2049. https://doi.org/10.1002/qj.3803
Hondula, D., Rocklöv, J., & Sankoh, O. (2012). Past, present, and future climate at select INDEPTH member health and demographic surveillance systems in Africa and Asia. *Global Health Action*, *5*(1), 19083. https://doi.org/10.3402/gha.v5i0.19083
Hong, S.-Y., & Lim, J.-O. J. (2006). The WRF single-moment 6-class microphysics scheme (WSM6). *Asia-Pacific Journal of Atmospheric Sciences*, *42*(2), 129–151.
Igri, P., Tanessong, R., Vondou, D., Panda, J., Garba, A., Mkankam, F., & Kamga, A. (2018). Assessing the performance of WRF model in predicting high-impact weather conditions over central and Western Africa: An ensemble-based approach. *Natural Hazards*, *93*(3), 1565–1587. https://doi.org/10.1007/s11069-018-3368-y
Ikeda, T., Behera, S., Morioka, Y., Minakawa, N., Hashizume, M., Tsuzuki, A., et al. (2017). Seasonally lagged effects of climatic factors on malaria incidence in South Africa. *Scientific Reports*, *7*(1), 1–9. https://doi.org/10.1038/s41598-017-02680-6
Jiang, A. L., Lee, M.-C., Zhou, G., Zhong, D., Hawaria, D., Kibret, S., et al. (2021). Predicting distribution of malaria vector larval habitats in Ethiopia by integrating distributed hydrologic modeling with remotely sensed data. *Scientific Reports*, *11*(1), 1–14. https://doi.org/10.1038/s41598-021-89576-8
Jiang, A. L., & Wang, K. (2019). The role of satellite-based remote sensing in improving simulated streamflow: A review. *Water*, *11*(8), 1617. https://doi.org/10.3390/w11081615
Kerandi, J. N., LauxLaux, P. J. P., Wagner, S., Kitheka, J., & Kunstmann, H. (2018). Joint atmospheric-terrestrial water balances for east Africa: A WRF-Hydro case study for the upper Tana River basin. *Theoretical and Applied Climatology*, *131*(3), 1337–1355. https://doi.org/10.1007/s00704-017-2050-8
Khaki, M. S. (2023). Land surface model calibration using satellite remote sensing data. *Sensors*, *23*(4), 1848. https://doi.org/10.3390/s23041848
Kibret, S., Wilson, G., Ryder, D., Tekie, H., & Petros, B. (2017). The influence of dams on malaria transmission in Sub-Saharan Africa. *EcoHealth*, *14*(2), 408–419. https://doi.org/10.1186/1475-2875-13-360
Kibret, S., Wilson, G., Tekie, H., & Petros, B. (2014). Increased malaria transmission around irrigation schemes in Ethiopia and the potential of canal water management for malaria vector control. *Malaria Journal*, *13*(1), 1–12. https://doi.org/10.1186/1475-2875-13-360
Klein, C., Heinzeller, D., Bliefernicht, J., & Kunstmann, H. (2015). Variability of West African monsoon patterns generated by a WRF multi-physics ensemble. *Climate Dynamics*, *45*(9), 2733–2755. https://doi.org/10.1007/s00382-015-2505-5
Lahmers, T., Gupta, H., Castro, C., Gochis, D., Yates, D., Dugger, A., et al. (2019). Enhancing the structure of the WRF-Hydro hydrologic model for semiarid environments. *Journal of Hydrometeorology*, *20*(4), 691–714. https://doi.org/10.1175/jhm-d-18-0064.1
Laneri, K., Bhadra, A., Ionides, E., Bouma, M., Dhiman, R., Yadav, R., & Pascual, M. (2010). Forcing versus feedback: Epidemic malaria and monsoon rains in Northwest India. *PLoS Computational Biology*, *6*(9), e1000898. https://doi.org/10.1371/journal.pcbi.1000898
Laux, P., Dieng, D., Portele, T., Arnault, J., Lorenz, C., Bliefernicht, J., & Kunstmann, H. (2021). A high-resolution regional climate model physics ensemble for Northern Sub-Saharan Africa. *Frontiers in Earth Science*, *9*. https://doi.org/10.3389/feart.2021.700249
Machault, V., Vignolles, C., Pages, F., Gadiaga, L., Tourre, Y., Gaye, A., et al. (2012). Risk mapping of anopheles gambiae S.L. densities using remotely-sensed environmental and meteorological data in an urban area: Dakar, Senegal. *PLoS One*, *7*(11), e50674. https://doi.org/10.1371/journal.pone.0050674
MacLeod, D., Jones, A., Di Giuseppe, F., Caminade, C., & Morse, A. (2015). Demonstration of successful malaria forecasts for Botswana using an operational seasonal climate model. *Environmental Research Letters*, *10*(4), 0440051. https://doi.org/10.1088/1748-9326/10/4/044005
Meng, C., Jin, H., & Zhang, W. (2023). Lateral terrestrial water flow schemes for the Noah-MP land surface model on both natural and urban land surfaces. *Journal of Hydrology*, *620*, 129410. https://doi.org/10.1016/j.jhydrol.2023.129410
Meyer Oliveira, A., Fleischmann, A., & Paiva, R. (2021). On the contribution of remote sensing-based calibration to model hydrological and hydraulic processes in tropical regions. *Journal of Hydrology*, *597*, 126184. https://doi.org/10.1016/j.jhydrol.2021.126184
Minakawa, N., Dida, G., Sonye, G., Futami, K., & Njenga, S. (2012). Malaria vectors in Lake Victoria and adjacent habitats in western Kenya. *PLoS One*, *7*(3), e32725. https://doi.org/10.1371/journal.pone.0032725
Mlawer, E. J., Taubman, S. J., Brown, P. D., Iacono, M. J., & Clough, S. A. (1997). Radiative transfer for inhomogeneous atmospheres: RRTM, a validated correlated-k model for the longwave (paper 97jd00237). *Journal of Geophysical Research-All Series*, *102*, 16–663.
Mohammadkhani, M., Khanjani, N., Bakhtiari, B., & Sheikhzadeh, K. (2016). The relation between climatic factors and malaria incidence in Kerman, South East of Iran. *Parasite Epidemiol Control*, *1*(3), 205–210. https://doi.org/10.1016/j.parepi.2016.06.001

Molineaux, L. (1988). The epidemiology of human malaria as an explanation of its distribution including some implications for its control. In W. H. Wernsdorfer & I. McGregor (Eds.), *Malaria, principles and practice of malariology* (pp. 913–998). Churchill Livingstone.

Morse, A., Doblas-Reyes, F. J., Hoshen, M., Hagedorn, R., & Palmer, T. (2005). A forecast quality assessment of an end-to-end probabilistic multi-model seasonal forecast system using a malaria model. *Tellus A: Dynamic Meteorology and Oceanography*, *57*(3), 464–475. https://doi.org/10.3402/tellusa.v57i3.14668

Moyo, E., Mhango, M., Moyo, P., Dzinamarira, T., Chitungo, I., & Murewanhema, G. (2023). Emerging infectious disease outbreaks in Sub-Saharan Africa: Learning from the past and present to be better prepared for future outbreaks. *Frontiers in Public Health*, *11*, 1049986. https://doi.org/10.3389/fpubh.2023.1049986

Musiime, A. K., Smith, D. L., Kilama, M., Rek, J., Arinaitwe, E., Nankabirwa, J. I., et al. (2019). Impact of vector control interventions on malaria transmission intensity, outdoor vector biting rates and Anopheles mosquito species composition in Tororo, Uganda. *Malaria Journal*, *18*(1), 445. https://doi.org/10.1186/s12936-019-3076-4

Mwakalinga, V. M., Sartorius, B. K., Limwagu, A. J., Mlacha, Y. P., Msellemu, D. F., Chaki, P. P., et al. (2018). Topographic mapping of the interfaces between human and aquatic mosquito habitats to enable barrier targeting of interventions against malaria vectors. *Royal Society Open Science*, *5*(5), 161055. https://doi.org/10.1098/rsos.161055

Naabil, E., Lamptey, B., Arnault, J., Olufayo, A., & Kunstmann, H. (2017). Water resources management using the WRF-Hydro modelling system: Case.study of the Tono dam in West Africa. *Journal of Hydrology: Regional Studies*, *12*, 196–209. https://doi.org/10.1016/j.ejrh.2017.05.010

Nachega, J., Uthman, O., Ho, Y.-S., Lo, M., Anude, C., Kayembe, P., et al. (2012). Current status and future prospects of epidemiology and public health training and research in the who African region. *International Journal of Epidemiology*, *41*(61), 1829–1846. https://doi.org/10.1093/ije/dys189

Ndugwa, R., Ramroth, H., Müller, O., Jasseh, M., Sié, A., Kouyaté, B., et al. (2008). Comparison of all-cause and malaria-specific mortality from two West African countries with different malaria transmission patterns. *Malaria Journal*, *7*(1), 15. https://doi.org/10.1186/1475-2875-7-15

Niu, G.-Y., Yang, Z.-L., Mitchell, K. E., Chen, F., Ek, M. B., Barlage, M., et al. (2011). The community Noah land surface model with multiparameterization options (Noah-MP): 1. Model description and evaluation with local-scale measurements. *Journal of Geophysical Research*, *116*, D12. https://doi.org/10.1029/2010JD015140

Nkumama, I. N., Oõmeara, W. P., & Osier, F. H. A. (2017). Changes in malaria epidemiology in Africa and new challenges for elimination. *Trends in Parasitology*, *33*(2), 128–140. https://doi.org/10.1016/j.pt.2016.11.006

Opoku, S., Leal Filho, W., Hubert, F., & Adejumo, O. (2021). Climate change and health preparedness in Africa: Analyzing trends in six African countries. *International Journal of Environmental Research and Public Health*, *18*(9), 4672. https://doi.org/10.3390/ijerph18094672

Ouedraogo, B., Inoue, Y., Kambiré, A., Sallah, K., Dieng, S., Tine, R., et al. (2018). Spatio-temporal dynamic of malaria in Ouagadougou, Burkina Faso, 2011–2015. *Malaria Journal*, *7*(1), 138. https://doi.org/10.1186/s12936-018-2280-y

Parihar, R. S., Kumar, V., Anand, A., Bal, P. K., & Thapliyal, A. (2024). Relative importance of VECTRI model parameters in the malaria disease transmission and prevalence. *International Journal of Biometeorology*, *68*(3), 495–509. https://doi.org/10.1007/s00484-023-02607-z

Pekel, J.-F., Cottam, A., Gorelick, N., & Belward, A. S. (2016). High-resolution mapping of global surface water and its long-term changes. *Nature*, *540*(7633), 418–422. https://doi.org/10.1038/nature20584

Pleim, J. E. (2007). A combined local and nonlocal closure model for the atmospheric boundary layer. part I: Model description and testing. *Journal of Applied Meteorology and Climatology*, *46*(9), 1383–1395. https://doi.org/10.1175/jam2539.1

Prince, S. D., Kerr, Y. H., Goutorbe, J. P., Lebel, T., Tinga, A., Bessemoulin, P., et al. (1995). Geographical, biological and remote sensing aspects of the hydrologic atmospheric pilot experiment in the Sahel (Hapex-Sahel). *Remote Sensing of Environment*, *51*(1), 215–234. https://doi.org/10.1016/0034-4257(94)00076-Y

Quenum, G. M. L. D., Arnault, J., Klutse, N., Zhang, Z., Kunstmann, H., & Oguntunde, P. (2022). Potential of the coupled WRF/WRF-Hydro modeling system for flood forecasting in the Ouémé River (West Africa). *Water*, *14*(8), 1192. https://doi.org/10.3390/w14081192

Ryan, S., Lippi, C., & Zermoglio, F. (2020). Shifting transmission risk for malaria in Africa with climate change: A framework for planning and intervention. *Malaria Journal*, *19*(1), 170. https://doi.org/10.1186/s12936-020-03224-6

Sadoine, M. L., Zinszer, K., Liu, Y., Gachon, P., Fournier, M., Dueymes, G., et al. (2024). Predicting malaria risk considering vector control interventions under climate change scenarios. *Scientific Reports*, *14*(1), 2430. https://doi.org/10.1038/s41598-024-52724-x

Sangaré, I., Ouattara, C., Soma, D., Soma, D., Assogba, B., Namountougou, M., et al. (2022). Spatial-temporal pattern of malaria in Burkina Faso from 2013 to 2020. *Parasite Epidemiol Control*, *18*, e00261. https://doi.org/10.1016/j.parepi.2022.e00261

Sauerborn, R. (2017). A gaping research gap regarding the climate change impact on health in poor countries. *European Journal of Epidemiology*, *32*(9), 855–856. https://doi.org/10.1186/s12940-017-0258-9

Senatore, A., Mendicino, G., Gochis, D. J., Yu, W., Yates, D. N., & Kunstmann, H. (2015). Fully coupled atmosphere-hydrology simulations for the central mediterranean: Impact of enhanced hydrological parameterization for short and long time scales. *Journal of Advances in Modeling Earth Systems*, *7*(4), 1693–1715. https://doi.org/10.1002/2015MS000510

Sie, A., Louis, V., Gbangou, A., Müller, O., Niamba, L., Stieglbauer, G., et al. (2010). The health and demographic surveillance system (HDSS) in Nouna, Burkina Faso, 1993–2007. *Global Health Action*, *3*(1), 5284. https://doi.org/10.3402/gha.v3i0.5284

Sié, A., Pflüger, V., Coulibaly, B., Dangy, J., Kapaun, A., Junghanss, T., et al. (2008). St2859 serogroup a meningococcal meningitis outbreak in Nouna health district, Burkina Faso: A prospective study. *Tropical Medicine and International Health*, *13*(6), 861–868. https://doi.org/10.1111/j.1365-3156.2008.02056.x

Silver, M., Karnieli, A., Ginat, H., Meiri, E., & Fredj, E. (2017). An innovative method for determining hydrological calibration parameters for the WRF-Hydro model in arid regions. *Environmental Modelling & Software*, *71*, 47–69. https://doi.org/10.1016/j.envsoft.2017.01.010

Skamarock, W. C., Klemp, J. B., Dudhia, J., Gill, D. O., Barker, D. M., Wang, W., & Powers, J. G. (2008). *A description of the advanced research WRF version 3 (No. NCAR/TN-475+STR) (Tech. Rep.)*. University Corporation for Atmospheric Research. https://doi.org/10.5065/D68S4MVH

Smith, D. L., Cohen, J., Chiyaka, C., Johnston, G., Gething, P., Gosling, R., et al. (2013). A sticky situation: The unexpected stability of malaria elimination. *Philosophical Transactions of the Royal Society B: Biological Sciences*, *368*(1623), 20120145. https://doi.org/10.1098/rstb.2012.0145

Smith, D. L., Willis, T., Alfieri, L., James, W., Trigg, M., Yamazaki, D., et al. (2020). Incorporating hydrology into climate suitability models changes projections of malaria transmission in Africa. *Nature Communications*, *11*(1), 4353. https://doi.org/10.1038/s41467-020-18239-5

Steinbach, S., Cornish, N., Franke, J., Hentze, K., Strauch, A., Thonfeld, F., et al. (2021). A new conceptual framework for integrating earth observation in large-scale wetland management in east Africa. *Wetlands*, *41*(7), 93. https://doi.org/10.1007/s13157-021-01468-9

Sullivan, D. (2010). Uncertainty in mapping malaria epidemiology: Implications for control. *Epidemiologic Reviews*, *32*(1), 175–187. https://doi.org/10.1093/epirev/mxq013

Tokarz, R., & Novak, R. (2018). Spatial-temporal distribution of anopheles larval habitats in Uganda using GIS/remote sensing technologies. *Malaria Journal*, *17*(1), 420. https://doi.org/10.1186/s12936-018-2567-z

Tompkins, A., Colón-González, F., Di Giuseppe, F., & Namanya, D. (2019). Dynamical malaria forecasts are skillful at regional and local scales in Uganda up to 4 months ahead. *Geohealth*, *3*(3), 58–66. https://doi.org/10.1029/2018GH000157

Tompkins, A., & Ermert, V. (2013). A regional-scale, high resolution dynamical malaria model that accounts for population density, climate and surface hydrology. *Malaria Journal*, *12*(65), 65. https://doi.org/10.1186/1475-2875-12-65

Tompkins, A., & Thomson, M. (2018). Uncertainty in malaria simulations in the highlands of Kenya: Relative contributions of model parameter setting, driving climate and initial condition errors. *PLoS One*, *13*(9), e0200638. https://doi.org/10.1371/journal.pone.0200638

Van Der Knijff, J., Younis, J., & De Roo, A. (2010). Lisflood: A gis-based distributed model for river basin scale water balance and flood simulation. *International Journal of Geographical Information Science*, *24*(2), 189–212. https://doi.org/10.1080/13658810802549154

Van de Vuurst, P., & Escobar, L. E. (2023). Climate change and infectious disease: A review of evidence and research trends. *Infectious Diseases of Poverty*, *12*(1), 51. https://doi.org/10.1186/s40249-023-01102-2

WHO. (2018). *World malaria report 2018 (Meeting report No. 210)*. World Health Organisations.

Wimberly, M., de Beurs, K., Loboda, T., & Pan, W. (2021). Satellite observations and malaria: New opportunities for research and applications. *Trends in Parasitology*, *37*(6), 525–537. https://doi.org/10.1016/j.pt.2021.03.003

Yamana, T., Bomblies, A., & Eltahir, E. (2016). Climate change unlikely to increase malaria burden in West Africa. *Nature Climate Change*, *6*(11), 1009–1013. https://doi.org/10.1038/nclimate3085

Yamana, T., & Eltahir, E. (2010). Early warnings of the potential for malaria transmission in rural Africa using the hydrology, entomology and malaria transmission simulator (hydremats). *Malaria Journal*, *9*(1), 1–10. https://doi.org/10.1186/1475-2875-9-323

Yamba, E. I., Fink, A. H., Badu, K., Asare, E. O., Tompkins, A. M., & Amekudzi, L. K. (2022). Climate drivers of malaria seasonality and their relative importance in Sub-Saharan Africa. *GeoHealth*, *7*(2), e2022GH000698. https://doi.org/10.1029/2022GH000698

Youssefi, F., Javad Valadan Zoej, M., Ali Hanafi-Bojd, A., Borahani Dariane, A., Khaki, M., & Safdarinezhad, A. (2022). Predicting the location of larval habitats of anopheles mosquitoes using remote sensing and soil type data. *International Journal of Applied Earth Observation and Geoinformation*, *108*, 102746. https://doi.org/10.1016/j.jag.2022.102746

Yucel, I., Onen, A., Yilmaz, K. K., & Gochis, D. J. (2015). Calibration and evaluation of a flood forecasting system: Utility of numerical weather prediction model, data assimilation and satellite-based rainfall. *Journal of Hydrology*, *523*, 49–66. https://doi.org/10.1016/j.jhydrol.2015.01.042

Zhang, J., Lin, P., Gao, S., & Fang, Z. (2020). Understanding the re-infiltration process to simulating streamflow in North Central Texas using the WRF-hydro modeling system. *Journal of Hydrology*, *587*, 124902. https://doi.org/10.1016/j.jhydrol.2020.124902

Zhang, Z., Arnault, J., Laux, P., Ma, N., Wei, J., & Kunstmann, H. (2021). Diurnal cycle of surface energy fluxes in high mountain terrain: High-resolution fully coupled atmosphere-hydrology modelling and impact of lateral flow. *Hydrological Processes*, *35*(12), e14454. https://doi.org/10.1002/hyp.14454